Journal of South American Earth Sciences 68 (2016) 167–186

Contents lists available at ScienceDirect

Journal of South American Earth Sciences

journal homepage: www.elsevier.com/locate/jsames

The Ediacaran Rio Doce magmatic arc revisited (Araçuaí-Ribeira orogenic system, SE Brazil)

Mahyra Tedeschi [a, c, *], Tiago Novo [a], Antônio Pedrosa-Soares [a, 1], Ivo Dussin [a, 1], Colombo Tassinari [b, 1], Luiz Carlos Silva [c], Leonardo Gonçalves [d], Fernando Alkmim [d, 1], Cristiano Lana [d], Célia Figueiredo [a], Elton Dantas [e, 1], Sílvia Medeiros [f], Cristina De Campos [g], Felipe Corrales [h], Mônica Heilbron [h, 1]

[a] Universidade Federal de Minas Gerais, Programa de Pós-Graduação em Geologia, IGC-CPMTC, Campus Pampulha, Av. Antônio Carlos 6627, 31270-901 Belo Horizonte, MG, Brazil
[b] Universidade de São Paulo, Instituto de Geociências, SHRIMP Laboratory, Cidade Universitária, Rua do Lago 562, 05508–080 São Paulo, SP, Brazil
[c] Serviço Geológico do Brasil (CPRM), Av. Brasil 1731, 30140–002 Belo Horizonte, MG, Brazil
[d] Universidade Federal de Ouro Preto, Departamento de Geologia, Campus do Morro do Cruzeiro, 35400-000 Ouro Preto, MG, Brazil
[e] Universidade de Brasília, Instituto de Geociências, Laboratório de Geocronologia, Asa Norte, 70910-900 Brasilia, DF, Brazil
[f] Universidade Federal do Rio de Janeiro, Instituto de Geociências, Departamento de Geologia, Av. Athos da Silveira Ramos 274, Ilha do Fundão, 21941-916 Rio de Janeiro, RJ, Brazil
[g] Univ. Munich, Germany, Dept. for Earth and Environmental Sciences - Ludwig-Maximilias-UniversitätMünchen, Theresienstr. 41/III. room, 340 - 80333 Munich, Germany
[h] Universidade do Estado do Rio de Janeiro, Departamento de Geologia Regional e Geotectônica, Rua São Francisco Xavier 524 Bloco A Sala 4001, Maracanã, 20559900 Rio de Janeiro, RJ, Brazil

ARTICLE INFO

Article history:
Received 1 July 2015
Received in revised form
31 October 2015
Accepted 20 November 2015
Available online 26 November 2015

Keywords:
Magmatic arc
Rio Doce arc
Araçuaí orogen
Ribeira belt
Mantiqueira province
Brasiliano

ABSTRACT

Described half a century ago, the Galiléia tonalite represents a milestone in the discovery of plate margin magmatic arcs in the Araçuaí-Ribeira orogenic system (southeastern Brazil). In the 1990's, analytical studies on the Galiléia tonalite finally revealed the existence of a Late Neoproterozoic calc-alkaline magmatic arc in the Araçuaí orogen. Meanwhile, the name Rio Doce magmatic arc was applied to calc-alkaline plutons found in the Araçuaí-Ribeira boundary. After those pioneer studies, the calc-alkaline plutons showing a pre-collisional volcanic arc signature and age between 630 Ma and 585 Ma have been grouped in the G1 supersuite, corresponding to the Rio Doce arc infrastructure. Here, we revisit the Rio Doce arc with our solid field knowledge of the region and a robust analytical database (277 lithochemical analyses, and 47 U–Pb, 53 Sm–Nd, 25 $^{87}Sr/^{86}Sr$ and 7 Lu–Hf datasets). The G1 supersuite consists of regionally deformed, tonalitic to granodioritic batholiths and stocks, generally rich in melanocratic to mesocratic enclaves and minor gabbroic to dioritic plutons. Gabbroic to dioritic enclaves show evidence of magma mixing processes. The lithochemical and isotopic signatures clearly reveal a volcanic arc formed on a continental margin setting. Melts from a Rhyacian basement form the bulk of the magma produced, whilst gabbroic plutons and enclaves record involvement of mantle magmas in the arc development. Tonalitic stocks (U–Pb age: 618–575 Ma, $\varepsilon Nd_{(t)}$: −5.7 to −7.8, Nd T_{DM} ages: 1.28–1.68 Ga, $^{87}Sr/^{86}Sr_{(t)}$: 0.7059–0.7118, and $\varepsilon Hf_{(t)}$: −5.2 to −11.7) form the northernmost segment of the Rio Doce arc, which dies out in the ensialic sector of the Araçuaí orogen. At arc eastern and central zones, several batholiths (e.g., Alto Capim, Baixo Guandu, Galiléia, Muniz Freire, São Vítor) record a long-lasting magmatic history (632–580 Ma; $\varepsilon Nd_{(t)}$: −5.6 to −13.3; Nd T_{DM} age: 1.35–1.80 Ga; $^{87}Sr/^{86}Sr_{(t)}$: 0.7091–0.7123). At arc western border, the magmatic evolution started with gabbro-dioritic and tonalitic plutons (e.g., Chaves pluton, U–Pb age: 599 ± 15 Ma, $\varepsilon Nd_{(t)}$: −4.8 to −6.8, Nd T_{DM} ages: 1.48–1.68 Ga, $^{87}Sr/^{86}Sr_{(t)}$: 0.7062–0.7068, and $\varepsilon Hf_{(t)}$: −4.3 to −9.7; and Brasilândia pluton, U–Pb age: 581 ± 11 Ma, $\varepsilon Nd_{(t)}$: −8.2 to −10.2, Nd T_{DM} ages: 1.63–1.68 Ga, $^{87}Sr/^{86}Sr_{(t)}$: 0.7088–0.7112, $\varepsilon Hf_{(t)}$: −12.3 to −14.9),

* Corresponding author. Universidade Federal de Minas Gerais, Programa de Pós-Graduação em Geologia, IGC-CPMTC, Campus Pampulha, Av. Antônio Carlos 6627, 31270-901 Belo Horizonte, MG, Brazil.
E-mail addresses: mahyratedeschi@gmail.com, mahyra.tedeschi@cprm.gov.br (M. Tedeschi).
[1] Fellow of the Brazilian Scientific Research Council (CNPq).

http://dx.doi.org/10.1016/j.jsames.2015.11.011

followed by late granodioritic intrusions (e.g., Guarataia pluton, U–Pb age: 576 ± 9 Ma, $\varepsilon Nd_{(t)}$: −12.52 to −13.11, Nd T_{DM} age: 1.74–2.06 Ga, $^{87}Sr/^{86}Sr_{(t)}$: 0.7104–0.7110, $\varepsilon Hf_{(t)}$: −12.9 to −21.6). The Muriaé batholith (U–Pb age: 620–592 Ma, $\varepsilon Nd_{(t)}$: −8.2 to −13.6, Nd T_{DM} age: 1.41–1.88 Ga) and the Conceição da Boa Vista (586 ± 7 Ma) and Serra do Valentim (605 ± 8 Ma) stocks represent a segment of the Rio Doce arc correlated to the Serra da Bolívia and Marceleza complexes, making the link between the Araçuaí and Ribeira orogenic domains. We suggest three phases of arc development: i) eastward migration of arc front (632–605 Ma), ii) widespread magma production in the whole arc (605–585 Ma), and iii) late plutonism in the western arc region (585–575 Ma). Usual processes of volcanic arc development, like subduction of oceanic lithosphere under a continental margin, followed by asthenosphere ascent related to slab retreating and break-off may explain the Rio Doce arc evolution.

1. Introduction

This paper focuses on a region that ranges from the northern to the central sectors of the Mantiqueira Province, encompassing the Araçuaí-Ribeira orogenic system (AROS). It includes two domains roughly limited by the 21°S parallel: the Araçuaí orogen, to the north, and the Ribeira belt, to the south (Fig. 1). The Araçuaí orogen and its counterpart located in Africa, the West Congo belt, represents the evolution of a confined orogenic system bounded by the São Francisco–Congo cratons along three sides and, to the south, connected to the Ribeira belt (Pedrosa-Soares et al., 2001, 2008; Alkmim et al., 2006). In contrast, the focused segment of the Ribeira belt had a much more complex evolution, involving the São Francisco-Congo and Paranapanema cratons, the southern Brasília belt, the Rio Negro magmatic arc, and the Búzios orogenic domain (Heilbron et al., 2008, 2013; Schmitt et al., 2008; Tupinambá et al., 2012; Trouw et al., 2013; Bento dos Santos et al., 2015). In this geotectonic scenario, the Rio Doce magmatic arc seems to represent a reliable link between the Araçuaí and Ribeira orogenic domains.

The knowledge on AROS granitic rocks significantly improved in the last two decades, after results of systematic geological mapping projects, carried out in the 1:100,000 and 1:50,000 scales, and the widespread use of lithochemical and isotopic (Sr, Nd, Hf) analyses, as well as U–Pb geochronology (e.g., Pedrosa-Soares et al., 2011; Valeriano et al., 2011; Tupinambá et al., 2012; Heilbron et al., 2013; Gonçalves et al., 2014, 2015; Gradim et al., 2014). This has led to the identification of several segments of Neoproterozoic magmatic arcs, related to distinct AROS evolution stages, crowning half a century of studies since the pioneer descriptions based only on field and microscope data came out.

In the early 1960's, the Galiléia tonalite, representing a "Late Proterozoic" batholith composed mainly by a foliated tonalite with melanocratic enclaves, was described in the Rio Doce river valley (Barbosa et al., 1964). More than thirty years later, detailed analytical studies of the Galiléia tonalite demonstrated its pre-collisional calc-alkaline affinity, leading to the interpretation of a volcanic arc formed on a continental plate margin around 595 Ma (Nalini Jr., 1997; Nalini Jr. et al., 2000). This magmatic arc, along with the discovery of Neoproterozoic ophiolite remnants, provided solid evidence to refute an exclusively ensialic evolution for the Araçuaí orogen (Pedrosa-Soares et al., 1992, 1998). Meanwhile, Rio Doce became the name of a calc-alkaline magmatic arc of "Neoproterozoic III" age, extending further to the south of the Galiléia tonalite, from latitude 20°–22° S (Figueiredo and Campos Neto, 1993). Since the late 1990's, geological maps produced by systematic mapping projects in the 1:100,000 and 1:50,000 scales have provided the cartographic basis that allow us to correlate lithological units for long distances with significant accuracy (e.g., Pinto et al., 2001; Pedrosa-Soares et al., 2003; Heilbron et al., 2007; Novo et al., 2010a; Paes et al., 2010).

After those studies, the calc-alkaline plutons showing a volcanic arc signature and age in the range of ca. 630–585 Ma have been grouped in the G1 supersuite of the Araçuaí orogen (Pedrosa-Soares et al., 2001, 2011). Recently, tonalitic and gabbroic plutons located in the northern Ribeira belt have been correlated to the G1 supersuite (Figueiredo, 2009; Novo, 2013; Heilbron et al., 2013; Corrales, 2015), including plutons ascribed to the Rio Doce arc by Figueiredo and Campos Neto (1993).

In the present paper, we revisit the Rio Doce magmatic arc through a robust analytical database (277 lithochemical analyses, and 47 U–Pb, 53 Sm–Nd, 25 $^{87}Sr/^{86}Sr$ and 7 Lu–Hf datasets), including new and compiled data from a great number of plutonic bodies ascribed to the G1 supersuite, together with solid field knowledge of the whole studied area.

2. Geological setting

The major lithotectonic assemblages found in the region of interest are (Fig. 2):

- ✓ The western Archaean–Palaeoproterozoic basement, representing the margin of the São Francisco paleocontinental region along the border of the lower plate (Pedrosa-Soares et al., 2001, 2008; Alkmim et al., 2006; Noce et al., 2007a,b);
- ✓ The eastern Palaeoproterozoic basement, including the Juiz de Fora, Pocrane and Quirino complexes (Noce et al., 2007a; Heilbron et al., 2010; Novo, 2013), representing the basement of the upper plate where the Rio Doce arc developed (Pedrosa-Soares et al., 2001, 2008; Alkmim et al., 2006);
- ✓ Neoproterozoic metavolcano-sedimentary and metasedimentary units, including the arc supracrustal units represented by the Rio Doce Group (Vieira, 2007; Pedrosa-Soares et al., 2008; Novo, 2013);
- ✓ Late Cryogenian to Early Ediacaran ophiolitic bodies (Pedrosa-Soares et al., 1992, 1998; Queiroga et al., 2007; Queiroga, 2010; Peixoto et al., 2015);
- ✓ The regional plutonic (G1 to G5) supersuites related to distinct tectonic stages of the orogenic evolution (Pedrosa-Soares et al., 2011), which are briefly described ahead.

From the oldest pre-collisional plutons to the emplacement of the latest post-collisional intrusions, the focused region records a long lasting (ca. 630–480 Ma) succession of granite production events (Pedrosa-Soares et al., 2011; Heilbron et al., 2013). We use the name granite in a general sense, if not otherwise specified. Regionally, the plutonic igneous rocks formed during the orogenic evolution stages have been grouped into five supersuites, namely G1, G2, G3, G4 and G5 (Pedrosa-Soares et al., 2011). Supersuites include suites, batholiths, stocks, and individual plutons, as well as minor igneous bodies like dikes, sills, veins and irregular-shaped

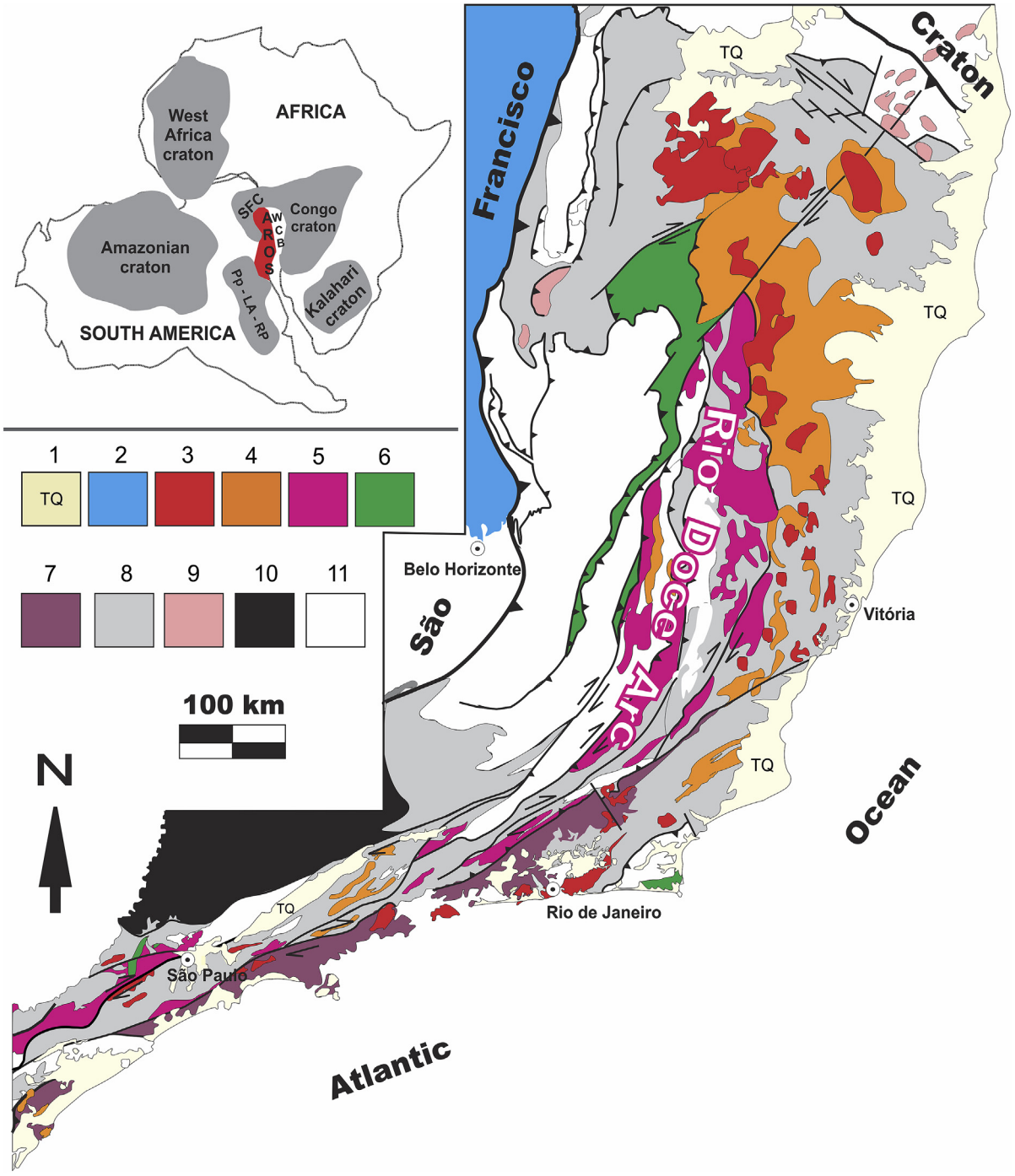

Fig. 1. Simplified geological map of the Araçuaí-Ribeira orogenic system (AROS) and its location in Western Gondwana (modified from Silva et al., 2005). 1, Cenozoic covers; 2, São Francisco craton covers. AROS units: 3, Post-collisional plutonism; 4, Collisional plutonism; 5, Rio Doce magmatic arc and probable correlatives; 6, Ophiolite-bearing rock assemblages; 7, Rio Negro arc domain; 8, Neoproterozoic metasedimentary and metavolcanic successions; 9, Tonian and Cryogenian rift-related magmatic rocks; 10, Southern Brasília belt; 11, Pre-Neoproterozoic units. WCB, West Congo belt. CSF, São Francisco craton. Pp-LA-RP, Paranapanema-Luiz Alves-Rio de La Plata cratonic blocks.

bodies (e.g., leucosomatic patches) of several sizes.

According to the data and references presented in the forthcoming items, the G1 supersuite corresponds to the plutonic portion of the Rio Doce magmatic arc (Fig. 2). It mostly consists of the expanded calc-alkaline series, represented by tonalites to granodiorites crowded with mafic to dioritic enclaves and facies, and minor gabbroic plutons. Regionally, G1 rocks show ductile deformation and metamorphism, although well-preserved igneous features are locally found (Nalini Jr. et al., 2000, 2005; Pedrosa-Soares et al., 2011). The G1 plutonic rocks clearly show a volcanic arc chemical signature and hybrid isotopic attributes, suggesting interaction between the Palaeoproterozoic continental basement and mantle derived magmas in a continental margin setting. The arc-related supracrustal deposits include metavolcano-sedimentary units of the Rio Doce Group in the arc domain (Vieira, 2007; Gonçalves et al., 2010; Novo, 2013), the Nova Venécia Complex in the back-arc region (Gradim et al., 2014) and metasedimentary deposits found in the fore-arc zone (Peixoto et al.,

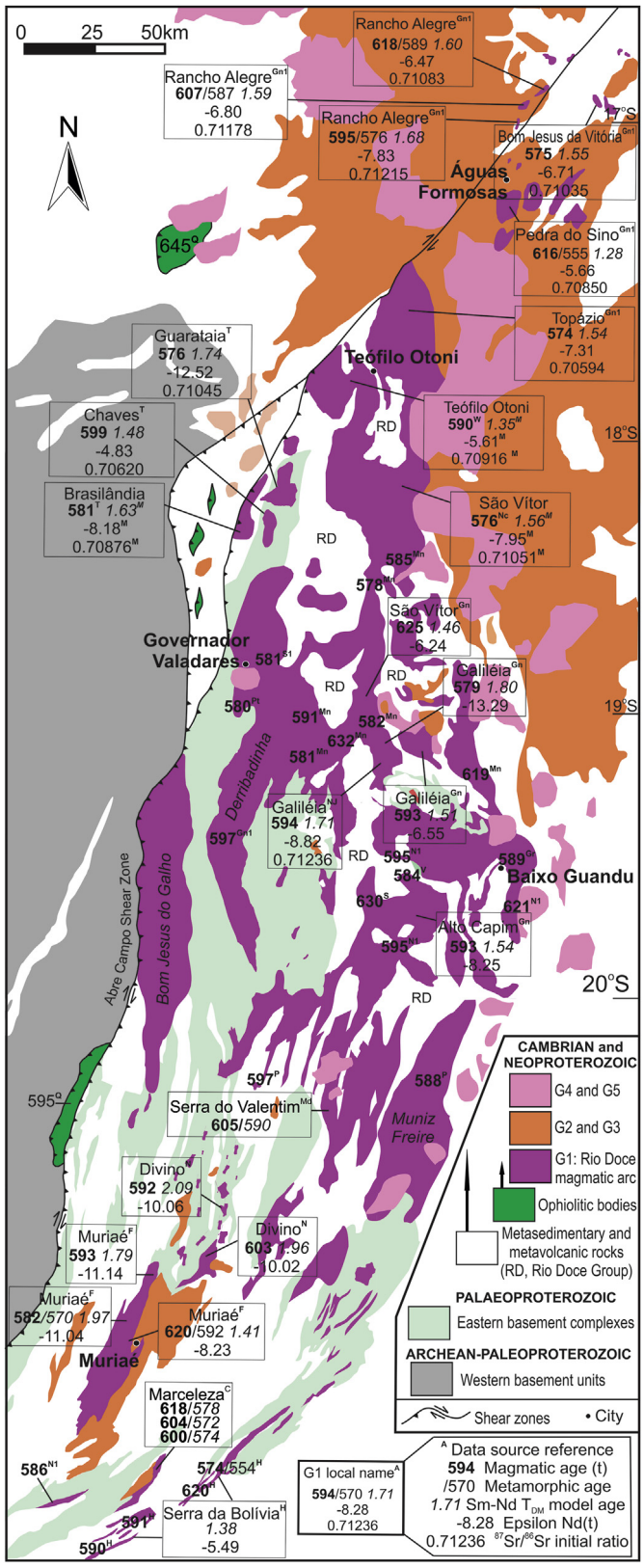

Fig. 2. Distribution of the main lithotectonic units of the Araçuaí-Ribeira orogenic system (modified from Pedrosa-Soares et al., 2007; Heilbron et al., 2013; Novo, 2013; and Gonçalves et al., 2015). Analytical data shown in the map are from: C, Corrales (2015); F, Figueiredo (2009); Gn, Gonçalves et al. (2014); Gn1, Gonçalves et al. (2015); Gr, Gradim et al. (2014); H, Heilbron et al. (2013); M, Martins et al. (2004); Mn, recalculated ages from Mondou et al. (2012); Md, Medeiros (this paper); N, Novo et al. (2010b); N1, Novo (2013); Nc, Noce et al. (2000); NJ, Nalini Jr. et al. (2000); P, Pedrosa-Soares et al. (2011); Pt, Petitgirard et al. (2009); Q, Queiroga (2010); S, Silva et al. (2005); S1, recalculated age from Silva et al. (2011); T, Tedeschi (2013); V, Vieira (2007); W, Whittington et al. (2001).

2015). G1 magmatism records an orogenic evolution from a pre-collisional to early collisional stages (ca. 630–580 Ma), associated with subduction of oceanic crust and convergence of the lower (São Francisco) plate against the upper (Congo) plate (Pedrosa-Soares et al., 2001; Alkmim et al., 2006; Heilbron et al., 2013; Gradim et al., 2014; Peixoto et al., 2015).

Although the G2 supersuite represents an essentially collisional granite population, the oldest G2 granites formed still in the pre-collisional stage of the Araçuaí orogen (Noce et al., 2000; Silva et al., 2002; Heilbron et al., 2013; Gradim et al., 2014). In fact, from the late pre-collisional to syn-collisional stages, the regional partial melting of Al-rich paragneisses produced a very large amount of peraluminous granites characteristic of the G2 supersuite (ca. 585–545 Ma; Pedrosa-Soares et al., 2011; Peixoto et al., 2015). G2 peraluminous granites form a continuous NS-trending belt, extending for over 350 km along AROS northeastern sector (Figs. 1 and 2). To the south, where deeper crustal levels are exposed, G2 granites occur in more restrict areas and smaller bodies (Pedrosa-Soares et al., 2003; Heilbron et al., 2007; De Campos et al., 2004; Gradim et al., 2014). Heat sources required to produce G2 magmas, in time and space, probably involved a complex combination of tectonic processes, like subduction of an ocean ridge, asthenosphere ascent under a hyper-extended back-arc, thrusting of the hot magmatic arc onto sedimentary deposits and increasing radioactive heat release related to collisional crustal thickening (Gradim et al., 2014; Bento dos Santos et al., 2015).

Late collisional to post-collisional crustal decompression, related to the fading of converging (tangential) stresses, associated to the radioactive thermal release of an over-thickened crustal pile, controlled the onset of a re-melting event, forming the mica-free cordierite-garnet leucogranites of the G3 supersuite (ca. 545–530 Ma). These leucogranites occur in veins, patches and small plutons grading to G2 granites (Gradim et al., 2014). Altogether, G2 and G3 granites represent a long lasting series of dehydrating melting processes, from ca. 585 Ma to ca. 530 Ma.

Finally, mantle delamination and gravity-driven tectonics caused a late orogenic extensional collapse, triggering the post-collisional production of magmas that formed the intrusions grouped into the G4 (ca. 530–500 Ma) and G5 (ca. 525–480 Ma) supersuites (Pedrosa-Soares et al., 2001, 2011; De Campos et al., 2004; and this volume; Belém, 2014; Gradim et al., 2014; Bento dos Santos et al., 2015). Muscovite-bearing peraluminous granites comprising the G4 intrusions are common in northern Araçuaí orogen (Pedrosa-Soares et al., 2011). The G5 supersuite includes balloon-like zoned plutons composed of granitic and mafic rocks, characterizing a bimodal plutonic assemblage. Outstanding features revealed by G5 plutons are diapir roots with inverse zoning (mafic cores and granitic borders), as well as widespread evidence of magma mixing. G5 intrusions cut across the regional structural trend, shaping the regional foliation around them. Although they are free from the regional foliation, they may show a local foliation developed along their margins owing to emplacement-related stresses (Wiedemann et al., 2002; De Campos et al., 2004; Gradim et al., 2014).

3. Analytical methods

We briefly synthesized the analytical methods used to obtain the new data here presented, which are the same described for

most data compiled from recent papers. Our samples were firstly cleaned (including removal of weathering coats and any other contaminants) and prepared (crushed and milled) for analyses in laboratories of the Universidade Federal de Minas Gerais (CPMTC-UFMG).

3.1. Lithochemichal analyses

Whole rock lithochemical analyses were conducted on 56 samples, taking into account the rock diversity of the G1 supersuite. Sample powders were analyzed by ACME and ACTLABS laboratories in Canada. Major and trace element contents were determined using Inductively Coupled Plasma–Atomic Emission Spectroscopy (ICP–AES) and Inductively Coupled Plasma–Mass Spectrometry (ICP–MS), respectively. Detection limits are 0.01% for oxides and 0.1 ppm for most trace elements, reaching values up to 0.01 ppm for Heavy Rare Earth Elements (HREE), such as Tb, Tm and Lu. New (56) and compiled (221) lithochemical analyses (277 samples) are available in the Supplementary data file labeled Lithochemical_Data.

3.2. U–Pb geochronological analyses

About 5–20 kg of each rock sample were prepared for analyses in laboratories of the Universidade de São Paulo and Universidade Federal de Ouro Preto, Brazil. Zircon grains were separated using conventional methods (crushing, grinding, gravimetric and magnetic-Frantz isodynamic separator) and handpicked under binocular microscope. For geochronological analysis of the magmatic rocks and their metamorphic equivalents, we selected zircon crystals from the least magnetic fractions. After mounted in epoxy disks and polished to expose grain centers, backscattered electron (BSE) and cathodoluminescence (CL) images revealed morphological features and internal structures of zircon grains. No analytical spot was performed on grain areas with inclusions, fractures and/or metamict features. U–Pb isotopic analyses were performed in the Sensitive High Resolution Ion Microprobe (SHRIMP) laboratories of the Universidade de São Paulo and Australian National University, as well as in Laser Ablasion Multi-collector Inductively Coupled Plasma Mass Spectrometry (LA-MC-ICP-MS) laboratories of the Brazilian universities of São Paulo, Brasília and Rio Grande do Sul, and the Ludwig-Maximilian Technical University of Munich. Temora (417 Ma; Black et al., 2003) and GJ-1 (Jackson et al., 2004) standard zircons were used in SHRIMP and LA-MC-ICP-MS analytical routines, respectively. In this study, the spot size in SHRIMP analyzes had 30 μm, and 25 μm in LA-MC-ICP-MS. Data reduction used the SQUID software (Ludwig, 2001) for the SHRIMP data, and the Excel sheet developed by Chemale et al. (2012) for the LA-MC-ICPMS data. Data evaluation for each spot took into account the common Pb contents, errors of isotopic ratios, percentages of discordance and Th/U ratios. From the selected spots, only those with discordance lesser than 10% were used to age calculations and plotted in Concordia diagrams. The Concordia diagram and histograms were obtained with the software Isoplot/Ex (Ludwig, 2003).

All new samples analyzed are from plutons of the G1 supersuite: five U–Pb (SHRIMP) analyses from samples M-02 (Chaves foliated gabbronorite), M-21 (Brasilândia foliated tonalite), M-11 (Guarataia granodiorite), TN-165 (Baixo Guandu tonalitic orthogneiss), MU-56 (Muriaé migmatitic orthogneiss granodioritic), and AR-6 (Conceição da Boa Vista tonalitic orthogneiss); and two U–Pb (LA-MC-ICP-MS) analyses from samples OPU-1415 (Serra do Valentin metagabbronorite) and CE-07 (foliated granite). The new U–Pb analyses are available in the Supplementary data file labeled U_Pb_data.

3.3. Sm–Nd and Rb–Sr analyses

Sm–Nd and Rb–Sr isotopic determinations were conducted at the Laboratory of Geochronology of Universidade de Brasília (UnB). Sm–Nd followed the method as described by Gioia and Pimentel (2000). Whole-rock powders (~50 mg) were mixed with a ^{149}Sm–^{150}Nd spike solution and dissolved in Savillex capsules. The lanthanides were extracted using ionic exchange conventional techniques in quartz columns using BIO-RAD-AG-50W-X8 resin. Sm and Nd extraction of whole-rock samples followed conventional cation exchange techniques, using Teflon columns containing LN-Spec resin di-(2-ethylhexyl) phosphoric acid (HDEHP) supported on PTFE powder. The fractions of Sr, Sm and Nd samples were loaded on re-evaporation filaments of double filament assemblies. The isotopic measurements were carried out on a multi-collector Finnigan MAT 262 mass spectrometer in static mode. Uncertainties for $^{87}Sr/^{86}Sr$ are smaller than 0.01% (2σ), and for Sm/Nd and $^{143}Nd/^{144}Nd$ ratios are better than ± 0.1% (2σ) and ±0.005% (1σ), respectively, based on repeated analyses of international rock standards BHVO-1 and BCR-1. $^{143}Nd/^{144}Nd$ ratios were normalized to $^{146}Nd/^{144}Nd = 0.7219$ and the decay constant (λ) used was $6.54 \times 10^{-12}y^{-1}$. T_{DM} ages were calculated according to DePaolo (1981).

We present sixteen new Sm–Nd analyses from the following G1 bodies: Chaves (M-02, foliated gabbronorite; L-12, L-22 and M-02W, foliated enderbite); Brasilândia (M-21A, foliated tonalite; M-21B and L-18, mafic enclaves); Guarataia (M-11, granodiorite), São Vítor (L-26A, foliated tonalite; L-26E and L-26C, mafic enclaves); Muriaé (CE-10, CE-56A, CE-76A and MU-56; hornblende-bearing orthogneisses; CE-57, foliated granite; CE-66B, mafic enclave). The five new Rb–Sr data are from samples M-02, M-02W, M-11, M-21A and M-21B. The new isotopic data are available in the Supplementary file labeled Isotopic_data.

3.4. Lu–Hf in zircon analyses

Besides the compiled Lu–Hf analyses in zircon, we present new data obtained via Laser Ablasion Multicollector Inductively Coupled Plasma Mass Spectrometry (LA-MC-ICP-MS, Photon machines 193/Neptune Thermo Scientific) at the Isotope Geochemistry Laboratory of the Universidade Federal de Ouro Preto, Brazil. Data were collected in static mode during 60s of ablation with a spot size of 50 μm. Nitrogen (~0.080 l/min) was introduced into the Ar sample carrier gas. Typical signal intensity was ca. 12 V for ^{180}Hf. The isotopes ^{172}Yb, ^{173}Yb and ^{175}Lu were simultaneously monitored during each analysis step to allow for correction of isobaric interferences of Lu and Yb isotopes on mass 176. The ^{176}Yb and ^{176}Lu were calculated using a $^{176}Yb/^{173}Yb$ of 0.796,218 (Chu et al., 2002) and $^{176}Lu/^{175}Lu$ of 0.02658 (JWG in-house value). The correction for instrumental mass bias utilized an exponential law and $^{179}Hf/^{177}Hf$ value of 0.7325 (Patchett and Tatsumoto, 1980) for correction of Hf isotopic ratios. The mass bias of Yb isotopes generally differs slightly from that of the Hf isotopes with a typical offset of the βHf/βYb of ca. 1.04 to 1.06 when using the $^{172}Yb/^{173}Yb$ value of 1.35,274 from Chu et al. (2002). This offset was determined for each analytical session by averaging the βHf/βYb of multiple analyses of the JMC 475 solution doped with variable Yb amounts and all laser ablation analyses (typically n > 50) of TEMORA zircon with a ^{173}Yb signal intensity of >60 mV. The mass bias behavior of Lu was assumed to follow that of Yb. The Yb and Lu isotopic ratios were corrected using the βHf of the individual integration steps (n = 60) of each analysis divided by the average offset factor of the complete analytical session. During analyses, secondary standards such as Plešovice, TEMORA, 91500 and GJ1 yielded $^{176}Hf/^{177}Hf$ ratios of 0.282475 ± 0.000010 (2σ, n = 09), 0.282661 ± 0.000011 (2σ, n = 04), 0.282299 ± 0.000017 (2σ, n = 07), and 0.282020 ± 0.000013

(2σ, n = 04), respectively. These ratios are in good agreement with the recommended values (e.g., Griffin et al., 2006; Wu et al., 2006; Morel et al., 2008; Sláma et al., 2008). The new Lu–Hf in zircon data come from the samples M-02 (Chaves foliated gabbronorite), M-21 (Brasilândia foliated tonalite) and M-11 (Guarataia granodiorite).

4. The Rio Doce magmatic arc

Figueiredo and Campos Neto (1993) suggested a first definition for the Rio Doce magmatic arc, including two series of "pre-collisional calc-alkaline plutonic rocks": the "tonalitic" and "enderbitic" series. This article is an important landmark for the characterization of the Rio Doce arc as the "tonalitic series" really includes pre-collisional plutons of the G1 supersuite, like Muniz Freire and Serra da Bolívia (De Campos et al., 2004; Pedrosa-Soares et al., 2011; Heilbron et al., 2013; and the present paper). However, the "enderbitic series" of Figueiredo and Campos Neto (1993) corresponds, in fact, to the peraluminous magmatism formed from the partial melting of metasedimentary gneisses (Sluitner and Weber-Diefenbach, 1989; Söllner et al., 1989; De Campos et al., 2004; Bento dos Santos et al., 2011; Gradim et al., 2014). Since then, the concept of Rio Doce arc has been used in distinct senses or even neglected possibly due to its relation to the controversial "Rio Doce orogeny" (Campos-Neto and Figueiredo, 1995).

Nevertheless, we consider the essence of the Rio Doce arc concept extremely useful nowadays, because it is the most important candidate to be a pre-collisional link between the Araçuaí and Ribeira orogenic domains. Furthermore, it records a singular case of a magmatic arc partially formed inside an inland-sea basin shaped like a large gulf, the confined Araçuaí-West Congo basin system. Therefore, we redefine the Rio Doce magmatic arc based on our solid fieldwork in the target region, as well as on a robust analytical database.

The Ediacaran Rio Doce magmatic arc includes the plutonic G1 supersuite and the metavolcano–sedimentary succession of the Rio Doce Group and correlatives (Fig. 2). The G1 supersuite mainly comprises tonalitic to granodioritic batholiths and stocks, rich in melanocratic to mesocratic enclaves, regionally deformed and metamorphosed during the Brasiliano orogeny, although locally showing well-preserved magmatic features (Pedrosa-Soares et al., 2011; Gonçalves et al., 2014, 2015; Heilbron et al., 2013; Novo, 2013; Tedeschi, 2013). Most enclaves are gabbro to diorite autoliths, suggesting magma mixing features. G1 supersuite also includes orthopyroxene-bearing (charnockitic) rocks, ranging in composition from gabbro to quartz monzonite (Novo et al., 2010b; Tedeschi, 2013; Gonçalves et al., 2014, 2015; Corrales, 2015). Metamorphosed pyroclastic and volcaniclastic rocks with dacitic to rhyolitic composition, intercalated in the lower Rio Doce Group, are supracrustal correlatives of the G1 supersuite. Additionally, the sedimentary deposits of this group also show remarkable evidence of provenance from the Rio Doce arc (Vieira, 2007; Gonçalves et al., 2010; Novo, 2013).

From north to south, the Rio Doce arc can be subdivided into three sectors: the northern sector comprising the G1 plutons located to the north of Teófilo Otoni; the central sector located between Teófilo Otoni and latitude 20° S; and the sector corresponding to the Araçuaí-Ribeira boundary, to the south of latitude 20° S (Fig. 2). From west to east, the arc encompasses three zones: the western border, a central zone and the eastern border, as we refer to in the next sections.

Structural and kinematic features of the Rio Doce arc central sector suggest an asymmetric, double–verging architecture, with the west–verging structures more developed than the east–verging ones. N–S–trending, W–verging thrusts mark the western boundary of the arc, whereas E–verging oblique thrusts and dextral strike–slip shear zones outline its eastern edge, and the internal region of the arc seems to be relatively preserved from large scale tectonic displacements and inversions (Alkmim et al., 2006; Gradim et al., 2014; Peixoto et al., 2015). To the north of latitude 18°30′S, some G1 plutons provide evidence that the arc died out in the ensialic region of the northern Araçuaí orogen (Gonçalves et al., 2015). To the south of latitude 20°S, in the Araçuaí-Ribeira boundary, NW–verging thrusts and remarkable NE-SW–trending, dextral strike-slip shear zones characterizes the evolution from the convergent to the docking stages of the orogenic evolution (Alkmim et al., 2006; Heilbron et al., 2008, 2010).

4.1. Lithochemical and isotopic overview

A large number (277) of lithochemical analyses from G1 plutons covers the studied region of the Rio Doce arc (Figs. 2 and 3). Besides our new data, a number of datasets compiled from the literature are available in a Supplementary file (Lithochemical_data). The compiled data came from distinct sources, published along the last 25 years. In most cases, field and petrographic descriptions allow us to check if the analyzed rock sample really belongs to the G1 magmatism. Nevertheless, it is important to take into account that the presented lithochemical dataset does not represent a single petrogenetic suite (in the sense of fractional crystallization), neither a batholith, nor a specific pluton at all. In fact, it is only a regional lithochemical overview of the Rio Doce magmatic arc (Fig. 3). Nevertheless, tendencies shown by this lithochemical overview agree with detailed studies carried out in distinct parts of the arc (Novo et al., 2010b; Heilbron et al., 2013; Tedeschi, 2013; Gonçalves et al., 2014, 2015; Corrales, 2015).

Regionally, lithochemical data from G1 rocks seems to disclose two compositional suites (referred to a decreasing order of abundance of their components). The most common suites, comprising tonalite, granodiorite, diorite, granite, gabbro-diorite and gabbro, occurs mainly in the central and eastern zones of the arc. The monzonitic suites, including quartz monzonite, monzodiorite, monzonite and monzogabbro, occurs mostly in the western zone of the arc. In both cases, these suites outline a general calc-alkaline trend in the AFM diagram, including very few tholeiitic terms (Fig. 3).

All together G1 granitic rocks are mostly (>80%) medium-to high-K in composition, although they significantly reach the shoshonite compositional field (<20%). Likewise, they are much more calcic to calc-alkaline and magnesian than alkali-calcic to alkaline and ferroan (Fig. 3).

Metaluminous to slightly peraluminous (<1.1 A/CNK; Fig. 3) granitic rocks largely prevail in the Rio Doce arc. Besides rock assemblages, mineralogical attributes and isotopic data, this lithochemical signature provides solid evidence that most G1 granitic rocks are equivalent to typical I-type magmas related to continental margin arcs (Wilson, 1989; Chappell and White, 2001; Chappell et al., 2012). Few data (<8%) suggest peraluminous rocks analogous to S-type granites (>1.1 A/CNK; Fig. 3). G1 samples with significantly peraluminous signatures are granitic rocks probably modified by assimilation of metapelite xenoliths, and late veins composed of garnet-bearing leucogranites.

5. Rio Doce arc – northern sector

Gonçalves et al. (2015) studied in detail the G1 plutons occurring in the northern termination of the Rio Doce magmatic arc, to the north of Teófilo Otoni (Fig. 2). We briefly summarize the results presented by those authors. According to zircon U–Pb data, the magmatic crystallization of those G1 plutons range from ca. 618 Ma to 574 Ma, including two age groups: plutons crystallized at

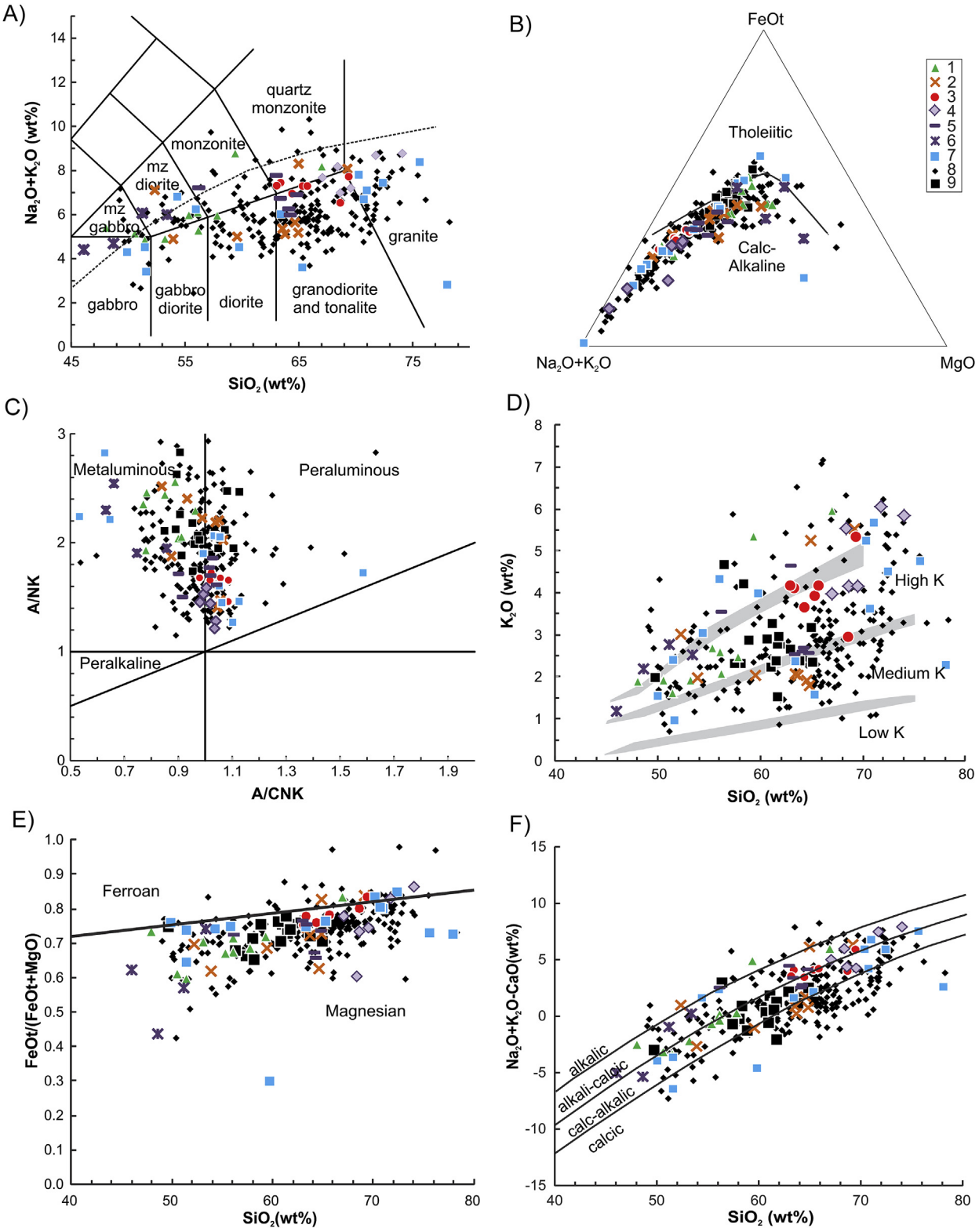

Fig. 3. Geochemical data from the Rio Doce Arc. A) Plot of $Na_2O + K_2O$ versus SiO_2 (wt.%) content (Wilson, 1989); B) AFM diagram (Irvine and Baragar, 1971); C) Variation of the Aluminium Saturation Index (A/CNK = mol. Al_2O_3/($CaO + Na_2O + K_2O$); Shand, 1943); D) K_2O versus SiO_2 (wt.%), subdivision of subalkaline rocks (Rickwood, 1989); E) FeO_{tot}/(FeO_{tot} + MgO) versus SiO_2 (wt.%) (Frost et al., 2001); F) Plot of $Na_2O + K_2O$–CaO (MALI) versus SiO_2 (wt. %) showing the spread distribution of the G1 rocks (Frost et al., 2001); Symbols: 1, Chaves Pluton; 2, Brasilândia Pluton; 3, Guarataia Pluton; 4, Muriaé Batholith granitic facies; 5, Muriaé Batholith hornblende gneiss facies; 6, Muriaé Batholith enclaves; 7, Manhumirim region between Baixo Guandu and Serra da Bolívia complex; 8, compiled data from the entire arc; 9, compiled data from the arc enclaves. Data from: Figueiredo and Campos-Neto (1993); Nalini Jr. (1997); Aracema et al. (1999); Vieira (2007); Gonçalves (2009); Novo et al. (2010b); Paes et al. (2010); Baltazar et al. (2010); Gonçalves et al. (2010); Heilbron et al. (2013); Gonçalves et al. (2014); Gonçalves et al. (2015); Medeiros (this work).

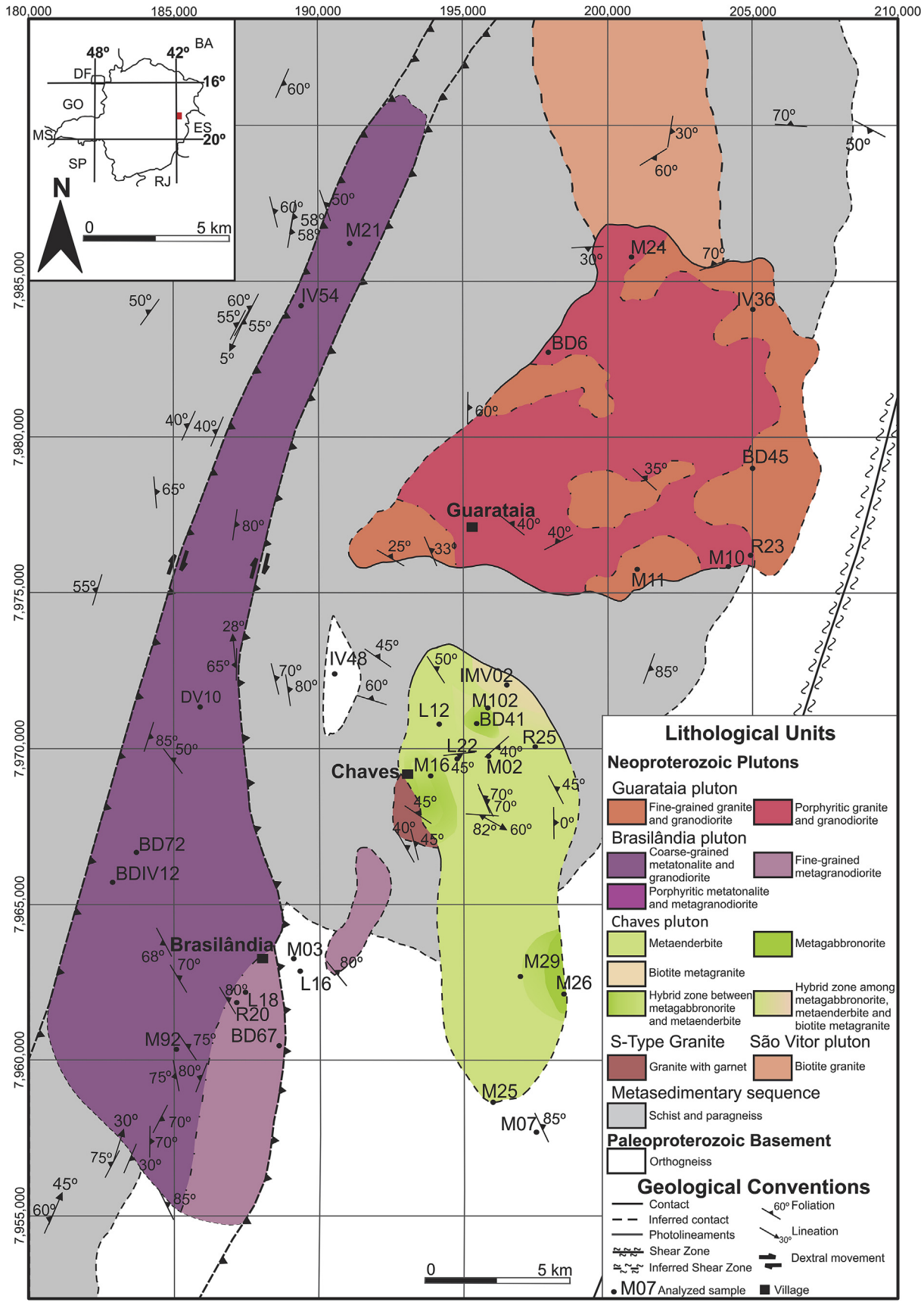

Fig. 4. Geological map of the Chaves–Brasilândia area, with indication of sample locations (Tedeschi, 2013).

618–595 Ma and migmatized at 589–555 Ma; and plutons crystallized around 575 Ma without evidence of migmatization. They consist of granodiorite, tonalite and monzogranite, similar to a magnesian, slightly peraluminous, calcic- (68%) to calc-alkaline (24%), medium-to high-K magmatic series (Fig. 3). Although marked by negative Nb, Ta, Sr and Ti anomalies, typically associated with subduction-related magmas, the combined isotopic data suggest a significant crustal contribution in magma genesis ($^{87}Sr/^{86}Sr_{(t)}$: 0.705939–0.712155; $\varepsilon Nd_{(t)}$: −5.7 to −7.8, $\varepsilon Hf_{(t)}$: −5.2 to −11.7; and Nd T_{DM} model ages: 1.4–1.7 Ga; Figs. 8 and 12).

When compared to the other segments of the Rio Doce arc, the northernmost G1 rocks show remarkable differences, as they are essentially slightly peraluminous granites (ASI = 1.07) relatively rich in biotite. According to Gonçalves et al. (2015), the northern plutons are not typical I-type or S-type granites, being particularly similar to granites of the Ordovician Famatinian arc (NW Argentina). Those authors suggest a hybrid model involving dehydration melting of meta-igneous (amphibolites) and metasedimentary (greywackes) rocks for magma production (Gonçalves et al., 2015).

6. Rio Doce arc – central sector: new data from a case study

After detailed field mapping of the western border of the Rio Doce magmatic arc, Tedeschi (2013) delimited three distinct G1 plutons, named Chaves, Brasilândia and Guarataia plutons (Fig. 4).

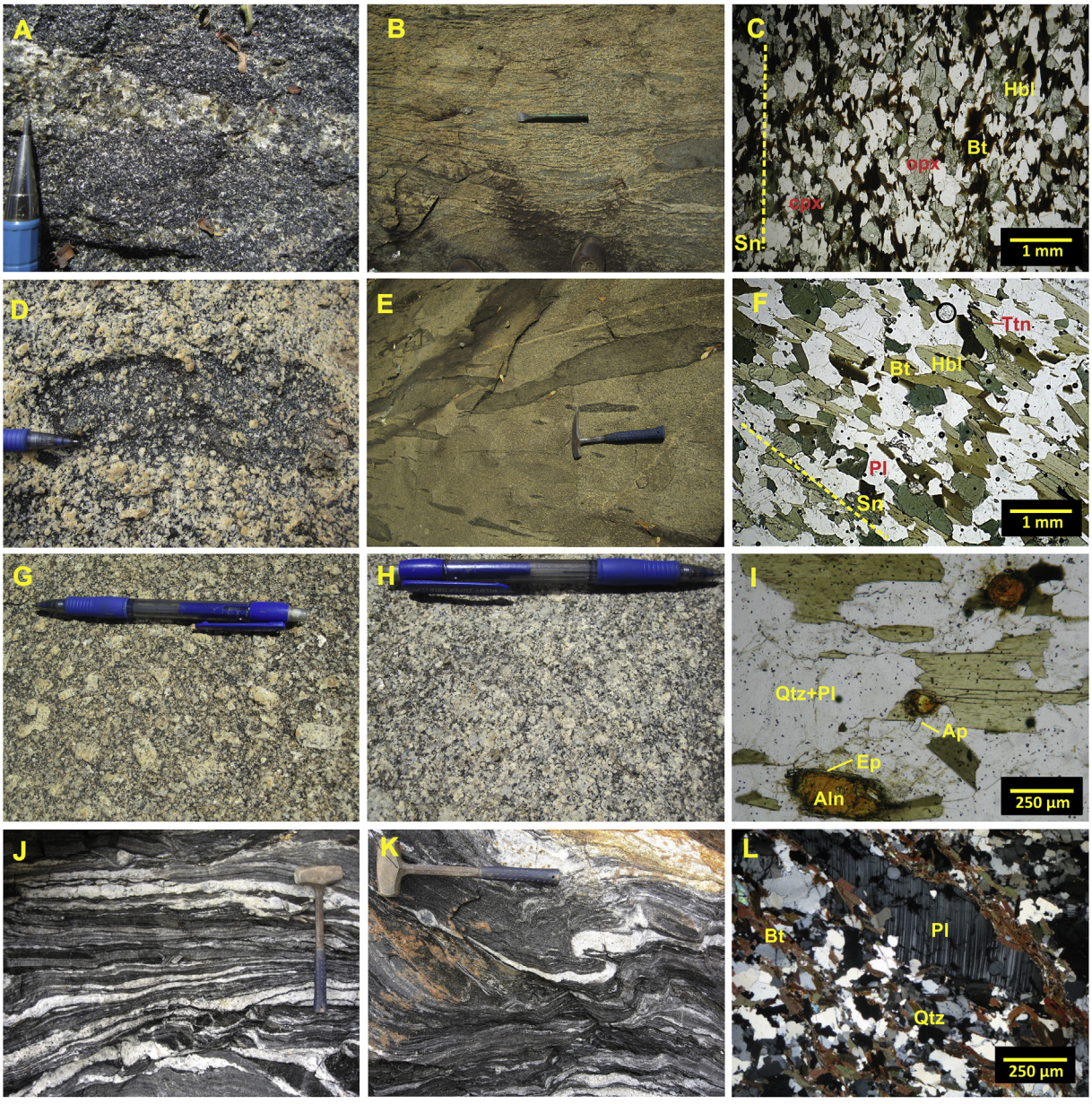

Fig. 5. Features of the central sector of the Rio Doce arc. A, gabbronorite with enderbite veins from Chaves pluton; B, stretched gabbronoritic enclaves in opdalitic rocks from Chaves pluton; C, photomicrograph of gabbronorite showing main mineral phases and the foliation; D, magma mixing feature from Brasilândia pluton: mafic dioritic enclave with plagioclase crystals from the coarse-grained tonalite matrix; E, stretched mafic enclaves with different homogenization degrees; F, photomicrograph of hornblende-biotite tonalite from Brasilândia foliated tonalite; G, porphyritic granite from Guarataia pluton; H, fine-grained granodiorite from Guarataia pluton; I, photomicrograph of a sample from the Guarataia pluton showing igneous flow marked by biotite, highlighting the abundance of allanite bordered by epidote; J, migmatitic gneiss from the Baixo Guandu batholith; K, migmatitic orthogneiss from Baixo Guandu batholith; E, photomicrograph from the migmatitic gneiss from Baixo Guandu batholith.

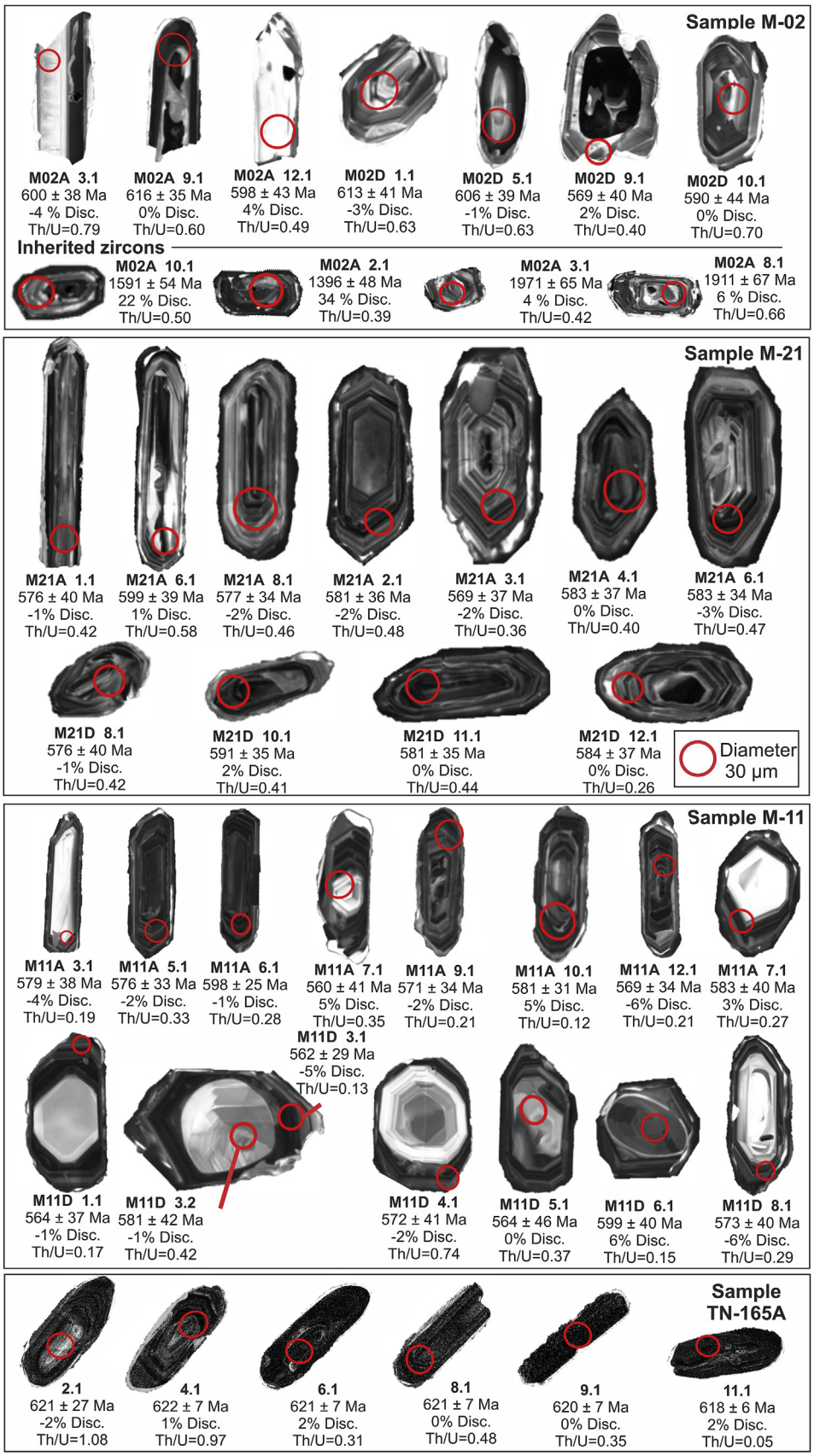

Fig. 6. Cathodoluminescence (CL) images from zircon grains. Samples M–02, M–11 and M–21 are from the Chaves–Brasilândia area (Fig. 4) and TN-165 from the eastern border of the Baixo Guandu batholith. Inherited zircons found in sample M–02 are also presented.

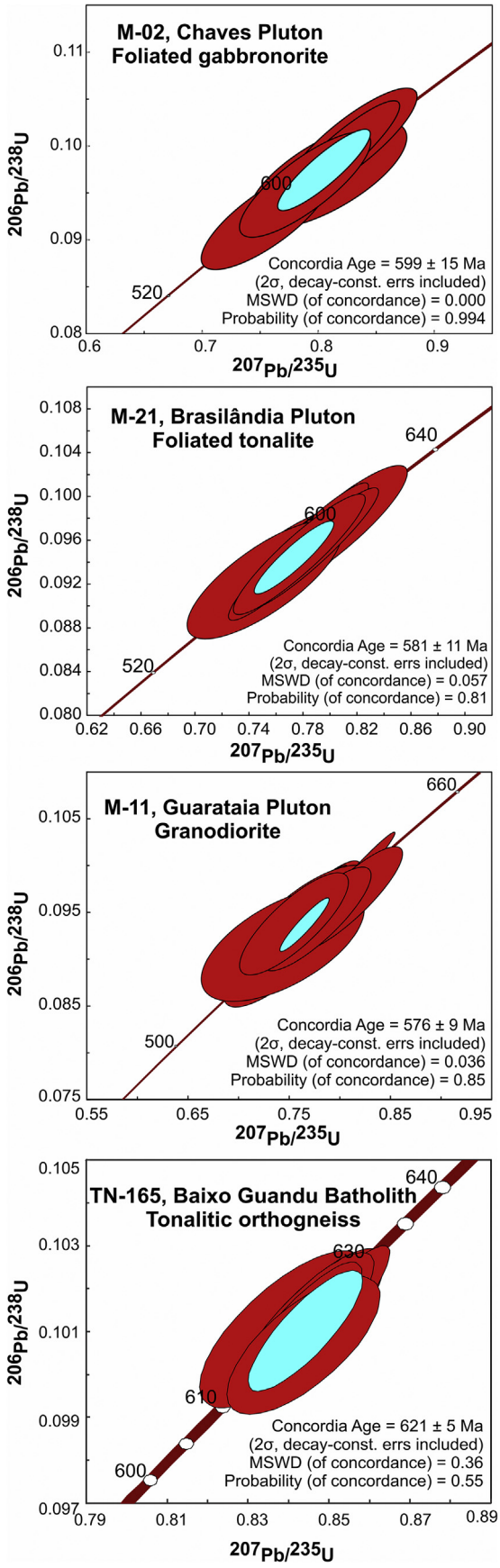

These plutons generally show the regional solid-state foliation superimposed in locally well-preserved magmatic fabrics.

6.1. Chaves pluton

It is a NS-trending elliptical body, showing a predominant enderbite facies, with minor gabbronorite, opdalite, charnockite, and biotite monzogranite facies (Figs. 4 and 5A to 5C). Contacts among those facies are transitional, marked by hybrid zones involving mixing of rocks from two or more facies (Fig. 5A to C). Gabbroic autoliths, and acicular apatite and amphibole growth over biotite plates are indicative of magma mixing processes (Hibbard, 1995).

Lithochemical data show a compositional trend from gabbro and tonalite to monzonite, with a magnesian, metaluminous, calc-alkaline (gabbroic rocks) to alkali-calcic (enderbitic to monzonitic rocks) signatures (Fig. 3).

Zircon populations extracted from a gabbronorite sample (M-02) consist of short-prismatic and elongated grains, ranging in length from 90 μm to 200 μm, with length/width ratios from 3:2 to 5:2, and few inherited rounded grains. Most grains are dark gray and display magmatic oscillatory zoning on CL images (Fig. 6). Analyzed spots yield only magmatic $^{232}Th/^{238}U$ ratios from 0.49 to 0.70. No grains show evidence of metamorphic overgrowth.

Seven spots of the sample M-02 yield a concordia age of 599 ± 15 Ma, interpreted as the crystallization age of the pluton (Fig. 7). Analyses of Lu–Hf isotopes in zircon spots yield Hf T_{DM} model ages from 1.47 to 1.75 Ga and $\varepsilon Hf_{(t)}$ from −4.31 to −9.66 (Fig. 8). These data together with the whole-rock Nd T_{DM} age (1.48 Ga), $\varepsilon Nd_{(t)}$ (−4.83) and $^{87}Sr/^{86}Sr_{(t)}$ (0.70620) suggest crustal contamination. In fact, four inherited zircon grains, with $^{207}Pb/^{206}Pb$ ages from ca. 2058 Ma to ca. 1875 Ma (Fig. 6), and $\varepsilon Hf_{(t)}$ of +1.94 and + 2.27, attest the contamination of the mafic magma by the Palaeoproterozoic basement. However, the least negative $\varepsilon Nd_{(t)}$ values, together with similar Nd and Hf isotope attributes of the gabbronorite facies are among the most primitive signatures yet found in the Rio Doce arc (cf. Martins et al., 2004; Pedrosa-Soares et al., 2011; Heilbron et al., 2013; Gonçalves et al., 2014, 2015).

Samples from the enderbitic (M-02W, L-12 and L-22) facies show Nd T_{DM} ages (1.57 and 1.58 Ga), $\varepsilon Nd_{(t)}$ (−4.90 to −6.78), and $^{87}Sr/^{86}Sr_{(t)}$ (0.70682), suggesting involvement of a major crustal component in magma genesis (Supplementary data files: Isotopic_data).

6.2. Brasilândia Pluton

The Brasilândia tonalite forms a NNE-trending sheet-shaped pluton limited by oblique thrust shear zones (Fig. 4). Locally, features of contact metamorphism on the host rock suggest intrusive emplacement prior to thrust development.

The pluton mainly consists of a foliated epidote-amphibole-biotite tonalite, with foliated epidote-amphibole-biotite granodioritic to granitic facies along its external zone, all of them rich in dioritic enclaves (Fig. 5D to F). Mafic to dioritic autoliths including plagioclase xenocrysts from the tonalite suggest magma mixing processes (Fig. 5D and E).

Lithochemical data reveal a continuous compositional trend from the gabbro-diorite enclaves (autoliths) to the late granitic facies, with the predominance of tonalite, showing a magnesian,

Fig. 7. U–Pb concordia diagrams for the Chaves foliated gabbronorite (sample M–02); Brasilândia foliated tonalite (sample M–21); Guarataia granodiorite (sample M–11); and Baixo Guandu tonalitic orthogneiss (sample TN-165).

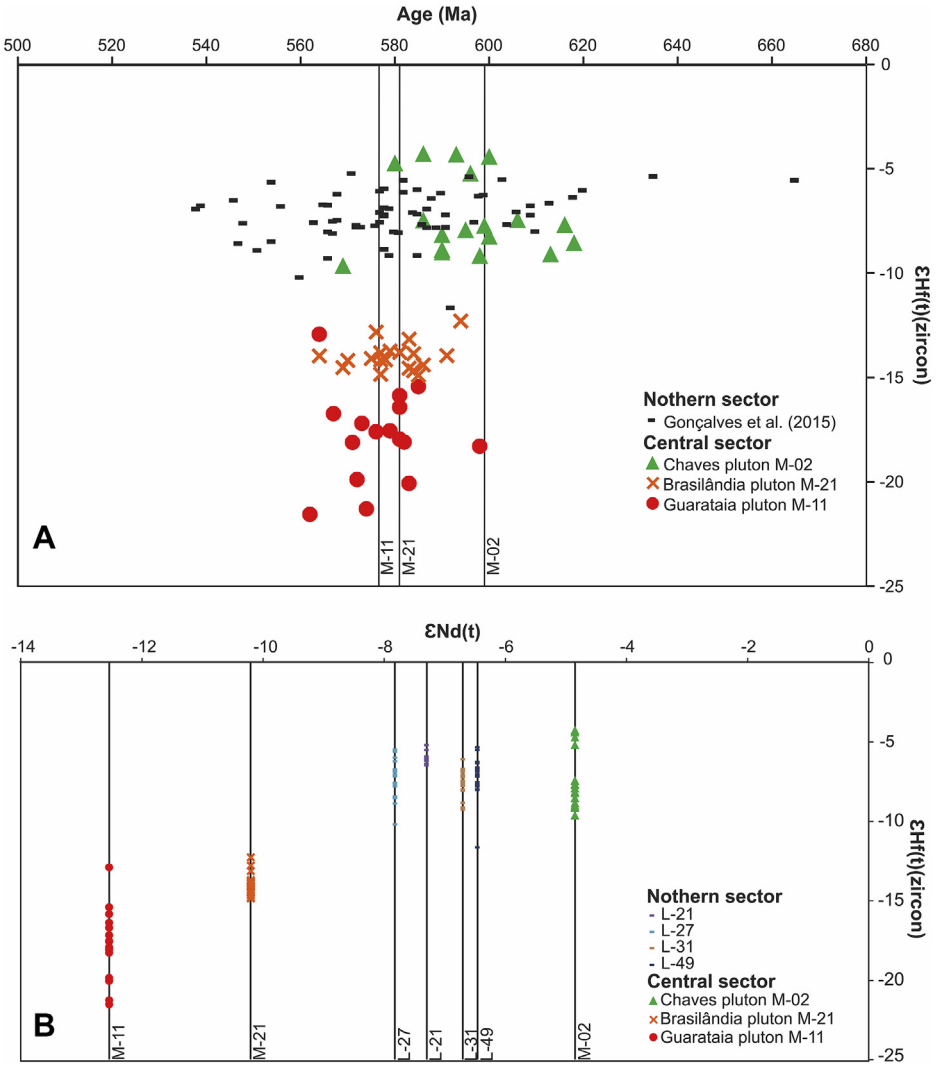

Fig. 8. Hf isotopic signature for the Rio Doce arc. A, Hf isotopic composition of zircon grains from the studied granitoids plotted against their age, together with the data from the northern sector from Gonçalves et al. (2015). B, Relationship between zircon εHf(t) and whole-rock εNd(t) for the northern (Gonçalves et al., 2015) and central sectors.

metaluminous to slightly peraluminous, medium-to high-K calc-alkaline signature. From core to border, the pluton evolves from calcic to alkaline terms (Fig. 3).

All zircon grains from a tonalite sample (M-21) are long to short prisms from 100 μm to 300 μm in length, and length/width ratios from 3:1 to 6:1, showing oscillatory zoning (Fig. 6). $^{232}Th/^{238}U$ ratios vary from 0.26 to 0.58. Eleven spots yield a concordia age of 581 ± 11 Ma for the magmatic crystallization of the Brasilândia pluton (Fig. 7).

Lu–Hf in zircon analyses from the tonalite sample (M-21) yield Hf T_{DM} ages from 1.9 Ga to 2.0 Ga, and $\varepsilon Hf_{(t)}$ from −12.30 to −14.89 (Fig. 8). This is in agreement with whole-rock Nd T_{DM} model ages around 1.7 Ga and $\varepsilon Nd_{(t)}$ values from −8.18 to −10.18 (Martins et al., 2004). Our analyses from enclaves yield Nd T_{DM} model ages from 1.78 Ga to 1.96 Ga, and $\varepsilon Nd_{(t)}$ from −8.20 to −9.13, as well as $^{87}Sr/^{86}Sr_{(t)}$ around 0.70641 which is the lowest value from this pluton (the highest $^{87}Sr/^{86}Sr_{(t)}$ ratio is 0.71119; Martins et al., 2004). Again, isotopic data suggest important crustal contribution for the genesis of a G1 tonalitic pluton of the Rio Doce arc.

6.3. Guarataia pluton

It is a roughly triangle-shaped pluton discordant of the regional structural trend, cutting across the Palaeoproterozoic basement, Neoproterozoic metasedimentary rocks and an older G1 pluton (São Vitor pluton; Fig. 4). Contrasting with Chaves and Brasilândia plutons, the Guarataia intrusion is largely free of the regional solid-state foliation. Having an isotropic core, the pluton shows features indicative of igneous flow and foliation along its borders.

It comprises fine-grained to coarse-grained porphyritic epidote-biotite granodiorite to granite, with mafic enclaves (Fig. 5G to I). Lithochemical analyzes show monzonite, granodiorite and granite compositions (Fig. 3). They are magnesian to ferroan, slightly peraluminous, and high-K calc-alkaline to alkali-calcic, similar to the peraluminous I-type granites (Chappell et al., 2012).

Zircon crystals from a sample (M-11) of the porphyritic granodiorite facies shows two distinct populations. The first includes short-prismatic grains, 150–300 μm in length, with most length/width ratios around 3:2. The second population consists of long-prismatic and large elongate grains, exhibiting length/width ratios from 4:1 to 5:2. The first population shows distinctive high luminescent cores, suggesting an apparent metamorphic recrystallization that was not corroborated by analyses on cores and rims. All grains display magmatic oscillatory zoning on CL images (Fig. 6). $^{232}Th/^{238}U$ ratios vary from 0.12 to 0.74.

Fourteen spot analyses from thirteen zircon grains yield a

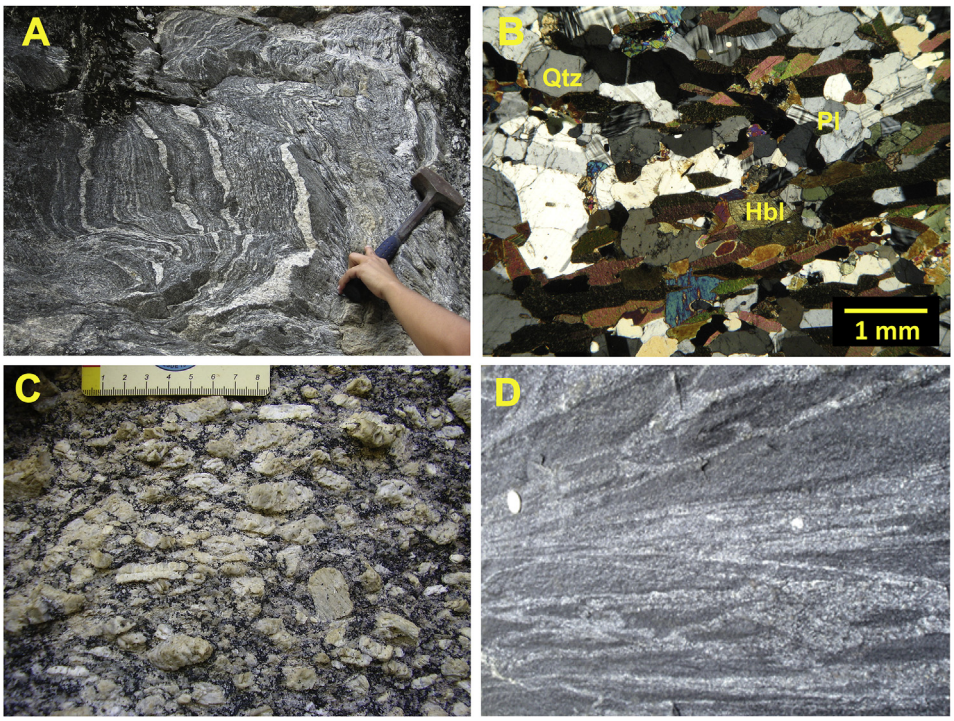

Fig. 9. Features of the southern sector of the Rio Doce arc. A, migmatitic hornblende orthogneiss from the Muriaé batholith; B-thin section of rock shown in A; C, porphyritic biotite granite from the Muriaé Batholith; D, amphibole-biotite gneiss with stretched gabbroic enclaves from the Conceição da Boa Vista tonalitic orthogneiss.

concordia age at 576 ± 9 Ma for the magmatic crystallization of the porphyritic granodiorite (Fig. 7). This age is very similar to the zircon Pb–Pb evaporation age of 575 ± 2 Ma, obtained by Noce et al. (2000) for the fine-grained granodiorite facies of the Guarataia pluton.

Results from Lu–Hf isotope analyses in zircon (Hf T_{DM} ages: 1.92 to 2.57 Ga; $\varepsilon Hf_{(t)}$: −12.91 to −25.02; Fig. 8) together with whole-rock Sm–Nd data (Nd T_{DM} ages: 1.74 Ga to 2.06 Ga, $\varepsilon Nd_{(t)}$: −12.52 to −13.11) and high $^{87}Sr/^{86}Sr_{(t)}$ ratios (0.71045–0.71099; Martins et al., 2004) are indicative of the crustal nature of the Guarataia pluton.

6.4. The Baixo Guandu batholith

Designated as Rio Guandu gneiss by Vieira (1993), the Baixo Guandu (or Mascarenhas) batholith was included in the G1 supersuite by Pedrosa Soares et al. (2001, 2011). Cropping out along the eastern arc border (Fig. 2), the Baixo Guandu batholith comprises tonalitic to granodioritic orthogneisses with stretched mafic to dioritic enclaves (autoliths). They also include xenoliths from the Rhyacian-Orosirian basement and Neoproterozoic metasedimentary rocks. The orthogneisses generally show migmatitic structures and ductile shear zones, suggesting that partial melting occurred during the collisional deformation (Novo, 2013; Gradim et al., 2014).

We present zircon U–Pb data for a sample (TN-165) from a tonalitic orthogneiss located at the eastern margin of the Baixo Guandu batholith (Fig. 5J). This rock is a strongly foliated, migmatitic, banded tonalitic orthogneiss rich in biotite (Fig. 5J to L). Zircon grains constitute a homogeneous population of prismatic crystals (ratio 2:1) with original igneous features, such as oscillatory zoning and high $^{232}Th/^{238}U$ (0.31–1.08), and some evidence of metamorphism, like thin metamorphic rims and $^{232}Th/^{238}U$ lower than 0.05 (Fig. 6).

One inherited zircon grain with igneous features ($^{232}Th/^{238}U$ = 0.75) yield a $^{207}Pb/^{206}Pb$ age of 835 ± 15 Ma, suggesting a contribution from a Tonian source in magma genesis. Regionally, similar ages have been found in detrital zircon spectra from Neoproterozoic metasedimentary covers on arc basement (Novo, 2013), and in igneous rocks of terrains located in the Ribeira belt (Cordani et al., 2002; Heilbron and Machado, 2003). On the other hand, this age coincides with a time gap found in the detrital zircon records for the precursor basin of the Araçuaí orogen (Kuchenbecker et al., 2015). Therefore, an explanation for the 835 Ma inherited zircon may be some assimilation of arc-related metasedimentary rocks during magma evolution, considering that the Baixo Guandu orthogneisses present xenoliths of those rocks.

Six U–Pb analyses yield a concordia age of 621 ± 5 Ma for the magmatic crystallization of the orthogneiss tonalitic protolith (Fig. 7). This is one of the oldest magmatic ages yet found in the Rio Doce arc (Fig. 2). To the north, a foliated tonalite records a much younger magmatic age (ca. 589 Ma, Gradim et al., 2014), suggesting a long-lasting magmatic history for the Baixo Guandu batholith.

7. The Rio Doce arc in the Araçuaí-Ribeira boundary: new data

Migmatization and strong deformation are common features in both G1 and basement orthogneisses along the sector to the south of latitude 20°S, where important strike-slip ductile shear zones overprinted previous thrusts. For this reason, some G1 bodies were interpreted as basement rocks (Quirino complex) in former publications (Noce et al., 2003; Tupinambá et al., 2007).

This is the region where the Rio Doce arc was defined (Figueiredo and Campos Neto, 1993). Actually, the Araçuaí-Ribeira connection arises from the correlation of the G1 bodies named Manhuaçu and Muniz Freire (Pedrosa-Soares et al., 2011), Serra do Valentim (this paper), Divino (Novo et al., 2010b), Muriaé (Figueiredo, 2009, and this paper), Conceição da Boa Vista (Novo, 2013, and this paper), Serra da Bolívia (Heilbron et al., 2013) and Marceleza (Corrales, 2015).

Fig. 10. Cathodoluminescence (CL) images of zircon grains from the Conceição da Boa Vista tonalitic orthogneiss (sample AR-6), migmatitic hornblende orthogneiss from the Muriaé batholith (sample MU-56), and metagabbronorite of the Serra do Valentim pluton (sample OPU-1415). Backscattered electron (BSE) images from zircon grains of the foliated granite from the Muriaé batholith (sample CE-07).

7.1. Serra do Valentim pluton

Formerly ascribed to the granulitic basement, the metamafic rocks found in the Serra do Valentim pluton were correlated to the Muniz Freire batholith by Figueiredo and Campos Neto (1992). We present new data supporting this correlation and assigning the Serra do Valentim gabbroic intrusion to the G1 supersuite of the Rio Doce arc.

The sample (OPU-1415) selected for U–Pb dating is a medium-grained metagabbronorite with an allotriomorphic texture, in which a net of mafic minerals (amphibole, pyroxene and biotite) has the spaces among them occupied by plagioclase and quartz. The zircon grains comprise short to medium-prismatic grains reaching 420 µm, with length/width ratios predominantly from 2:1 to 5:2 (Fig. 10). The CL images reveal interesting internal structures which depict a more or less dark inner domain and a light outer domain. The inner domain shows broad zoning and euhedral outer shape. In every case the outer domain, which is light in luminescence, has

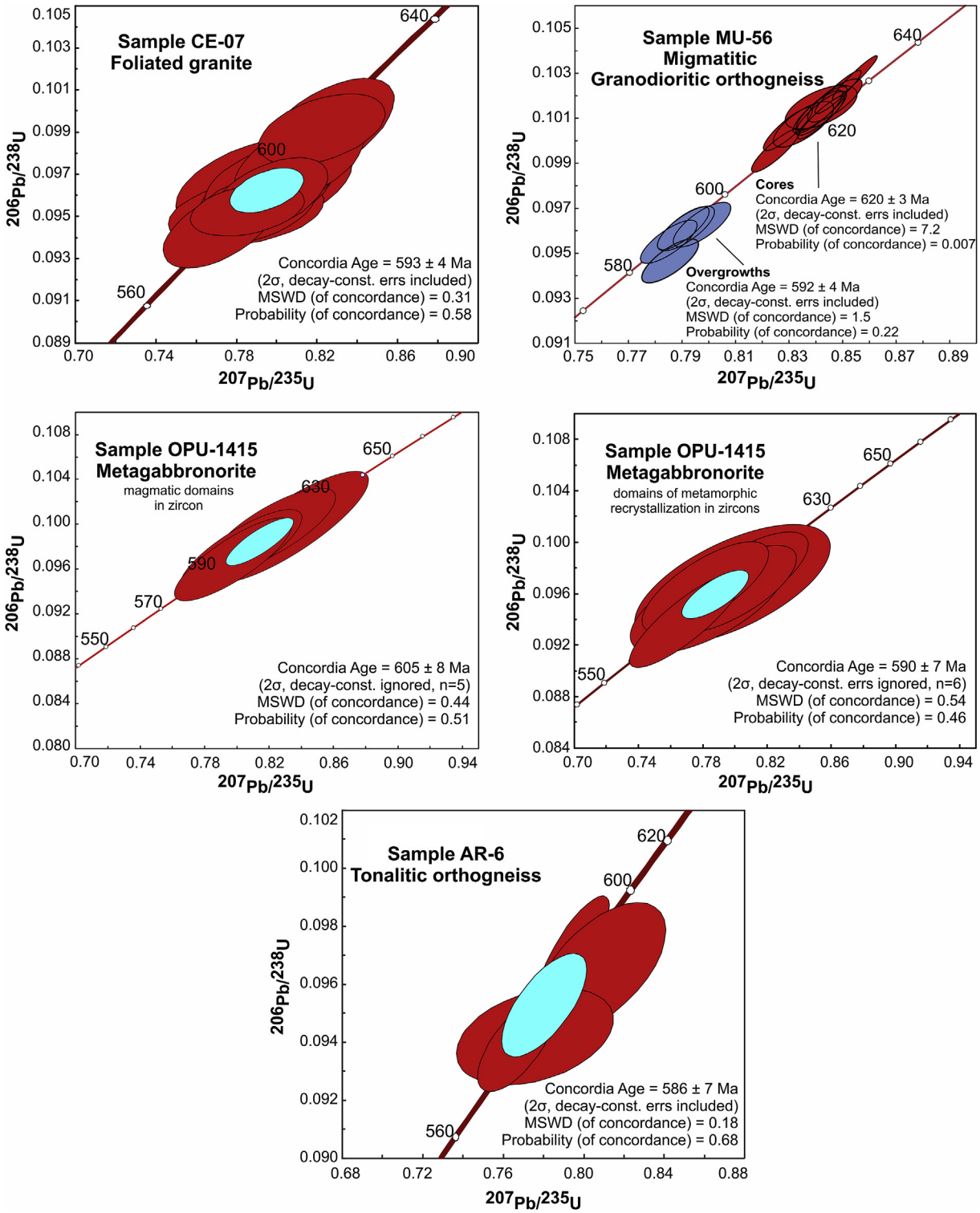

Fig. 11. U–Pb concordia diagrams for plutons from the southern sector of the Rio Doce arc. Muriaé foliated granite (sample CE-07); Muriaé migmatitic hornblende gneiss (sample MU-56); Serra do Valentim pluton (sample OPU-1415); Conceição da Boa Vista tonalitic gneiss (sample AR-6).

curved, bay like, convex boundaries to the inner domain, indicating recrystallization (Fig. 10). The grains have Th/U ratios ranging from 0.72 to 2.47, all suggesting a magmatic origin.

Five spots from six zircon grains yield a concordia age of 605 ± 8 Ma (Fig. 11), which is the best time constraint for the magmatic crystallization of the Serra do Valentim gabbronorite. Six spots from the outer domains yield a concordant age of 590 ± 7 Ma (Fig. 11), interpreted as the age of a metamorphic event.

7.2. Muriaé Batholith

Based on lithological correlation, Noce et al. (2003) and

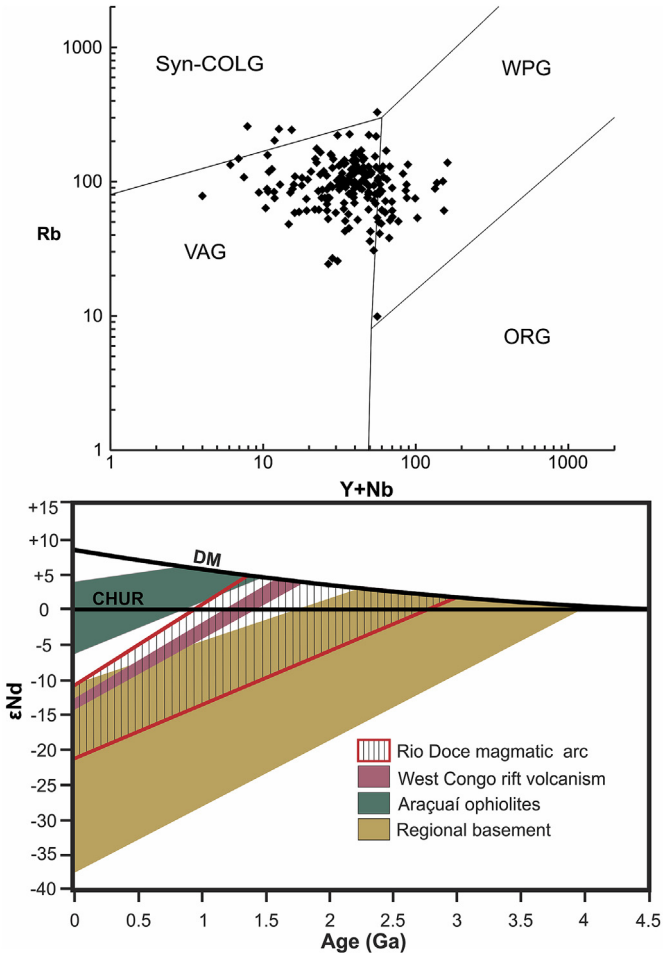

Fig. 12. Tectonic lithochemical diagram for Rio Doce arc (after Pearce et al., 1984; data sources in Fig. 3). Nd isotopic evolution diagram for the Rio Doce arc. Data sources: Pedrosa-Soares et al. (1998); Nalini Jr. et al. (2000); De Campos et al. (2004); Martins et al. (2004); Queiroga et al. (2007); Noce et al. (2007a); Figueiredo (2009); Gonçalves (2009); Novo et al. (2010b); Queiroga (2010); Gonçalves-Dias (2012); Pedrosa-Soares et al. (2011); Heilbron et al. (2013); Novo (2013); Tedeschi (2013); Gonçalves et al. (2014); Gonçalves et al. (2015).

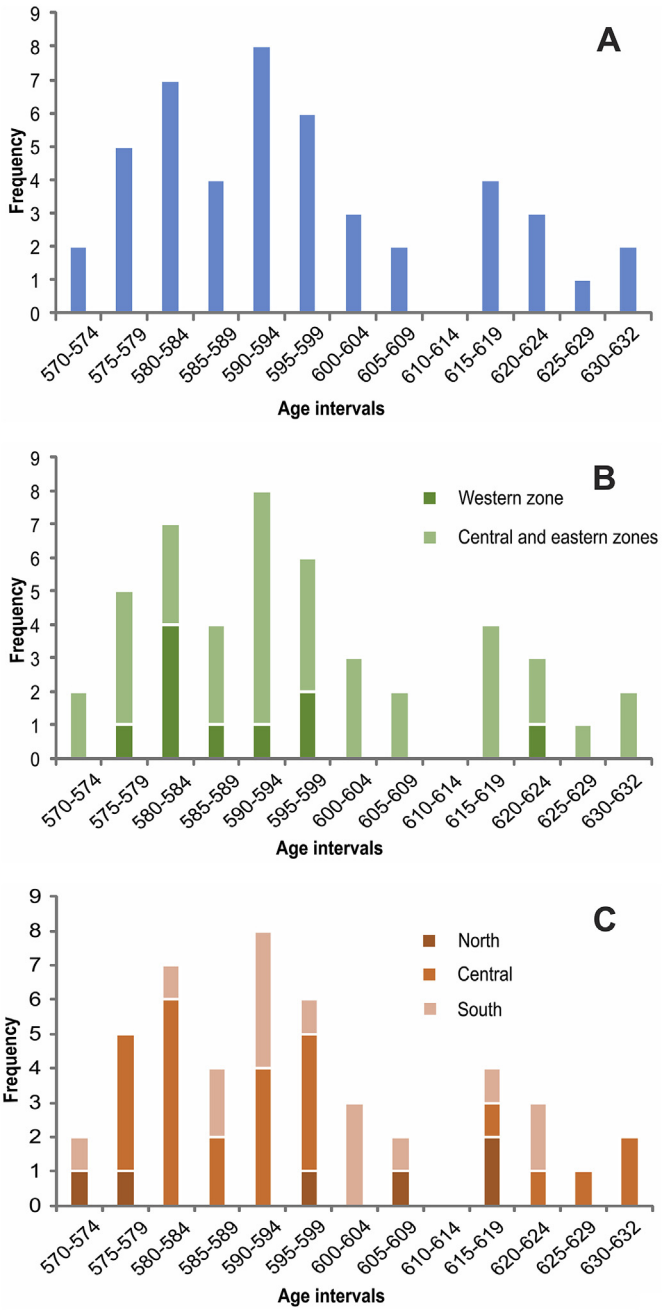

Fig. 13. U–Pb age distribution histograms for the Rio Doce arc. A, general age diagram; B, diagram highlighting the western, and central and eastern arc zones; C, diagram highlighting the northern, central and southern arc sectors (data sources referred in Fig. 2 caption).

Tupinambá et al. (2007) assigned the Muriaé migmatitic orthogneisses to the Palaeoproterozoic Quirino Complex. After U–Pb data, Figueiredo (2009) ascribed the same rocks to the G1 supersuite, redefining the Muriaé batholith. It is an extremely deformed body, elongated along the NE–SW structural trend, including migmatitic hornblende orthogneiss (Fig. 9A to C), and minor allanite-magnetite-bearing foliated granite and leucocratic granite. The last two granites are free of migmatization and represent a late stage of the batholith evolution (Fig. 8A). Lithochemical data indicate monzonitic to granitic compositions with a high-K calc-alkaline to alkali-calcic, metaluminous to slightly peraluminous signature (Fig. 3).

The selected sample (MU-56A) is a migmatitic hornblende-bearing orthogneiss, composed of granodioritic paleosome and granitic neosome. It furnished prismatic zircon grains ranging from 170 to 500 μm in length, with length/width ratios around 2:1 (Fig. 9A and B). Most of them show distinctive low luminescent zoned cores with $^{232}Th/^{238}U$ between 0.04 and 0.18, surrounded by high luminescent rims, generally showing oscillatory zoning with $^{232}Th/^{238}U$ from 0.20 to 0.52 (Fig. 10). Zircon grains from the granodioritic paleosome do not exhibit evidence of overgrowth, whilst those from the granitic neosome show clear overgrowth rims (Fig. 10, spots 2.2, 3.2, 5.1, 6.1, 11.2, 17.2). Twelve spot analyses on cores yield a mean $^{206}Pb/^{238}U$ age of 620 ± 3 Ma, interpreted as the magmatic crystallization age for the granodioritic paleosome. Six spots performed on grain rims yield a concordia age of 592 ± 4 Ma, assumed as the crystallization age of zircon overgrowths related to the intense migmatization shown in the outcrop (Fig. 11). Two inherited grains yield ages around 670 Ma (Fig. 10). They may be explained by magmatic assimilation of arc-related supracrustal rocks, which contain many zircon grains with similar ages (Novo, 2013), during the granodioritic magma evolution.

A sample (CE-07) represents the foliated porphyritic biotite granite of the Muriaé batholith (Fig. 9C). The zircon crystals can be

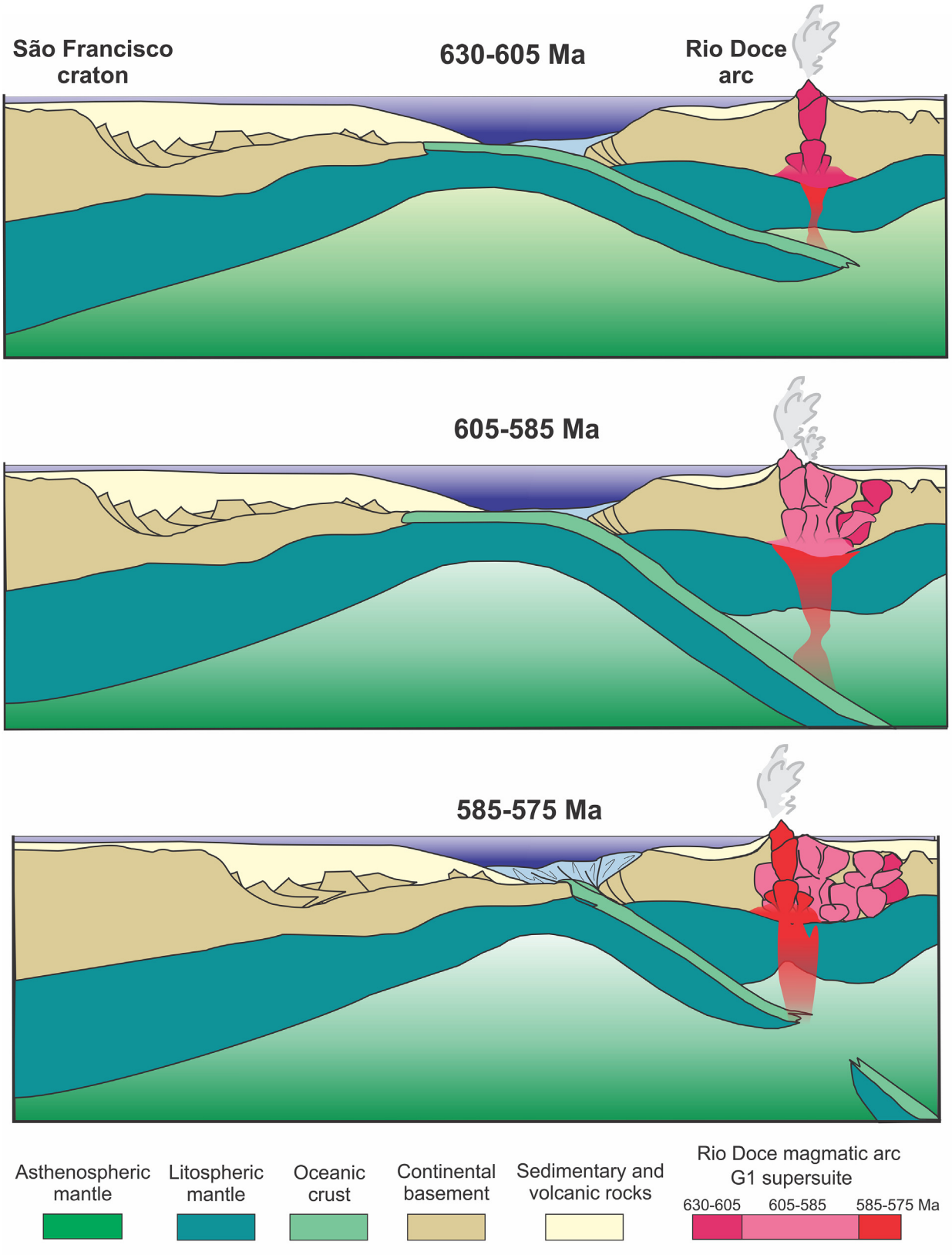

Fig. 14. Evolutionary model for the central sector of the Rio Doce magmatic arc (not to scale).

grouped into a predominant population (elongated prisms, 100 μm in length, with length/width ratios greater than 3:1), and a minor group (shorter prisms, with length/width ratios around 7:3 and poorly developed shapes). Most grains exhibit internal zoning and $^{232}Th/^{238}U$ ratios ranging from 0.07 to 1.54 (Fig. 10). Twelve spots yield a $^{206}Pb/^{238}U$ age of 593 ± 4 Ma for the magmatic crystallization of the porphyritic granite (Fig. 11).

Sm–Nd analyses on whole-rock samples from the migmatitic hornblende orthogneiss paleosome provide Nd T_{DM} model ages from 1.41 Ga to 1.88 Ga, and $\varepsilon Nd_{(620)}$ from −8.23 to −10.99. The late granite shows a Nd T_{DM} model age at 1.83 Ga and $\varepsilon Nd_{(593)}$ of −13.59. Both rocks record the continental basement contribution for their magmatic protoliths.

7.3. Conceição da Boa Vista tonalite

Formed by tectonic slices interleaved with rocks of the basement and metasedimentary cover, grading to strongly deformed migmatitic terms, this tonalitic orthogneiss was ascribed to the Palaeoproterozoic Quirino complex (Tupinambá et al., 2002). However, Novo (2013) assigned the Conceição da Boa Vista tonalitic orthogneiss to the G1 supersuite after the new U–Pb data presented ahead.

The selected sample (AR-6), a hornblende-biotite tonalitic orthogneiss with stretched gabbroic enclaves (Fig. 9D), furnished elongated (3:1) prismatic zircon crystals with oscillatory zoning and $^{232}Th/^{238}U$ ratios from 0.04 to 1.17. Three inherited zircons (2132 ± 7 Ma, 2029 ± 5 Ma and 2012 ± 16 Ma; Fig. 10) attested basement involvement in magma production (Heilbron et al., 2010). Four spots yield a concordia age of 586 ± 7 Ma, interpreted as the magmatic crystallization age for the tonalitic protolith (Fig. 11).

8. Discussion and conclusion

The Rio Doce magmatic arc extends at least for some 550 km from the northern sector of the Araçuaí orogen to the Ribeira orogenic belt, roughly between latitudes 17° and 22° S, i.e., more than 100 km to the south of the conventional Araçuaí-Ribeira boundary (Figs. 1 and 2). It reaches its maximum width around 140 km in the central sector, at Baixo Guandu latitude, which represents the most complete remnant sector of the formerly full-developed arc. Owing to the present-day erosional levels, exposures of the arc infrastructure, represented by the G1 supersuite, are much more common than its volcano-sedimentary cover, recorded by the lower formations of the Rio Doce Group.

The G1 rock assemblages, similar to an expanded calc-alkaline series, together with robust lithochemical and isotopic datasets strongly suggest a pre-collisional magmatic arc developed on an active continental margin setting (Figs. 3, 8 and 12). Isotopic (whole-rock Nd and Sr, and Hf in zircon) data reveal an important contribution of continental crust in arc genesis (Figs. 8 and 12). Indeed, the contribution of the crustal basement might be very important, as one expects for magmatic arcs developed on continental margins. Furthermore, a great part of the Rio Doce arc formed inside a confined orogenic setting, the Araçuaí orogen, where the continental crust would be much more extensive than the oceanic crust. The εNd evolution diagram clearly shows the very significant contribution of the continental crust, mostly represented by the Rhyacian-Orosirian basement and anorogenic igneous rocks of the precursor rift system (Fig. 12). Most Nd model ages, ranging from 1.2 Ga to 2.0 Ga, also reflect the mixture of older continental sources with relatively younger sources. The last can be related to the Neoproterozoic rift-related magmatism and, at least in part, to some influence of the Cryogenian–Ediacaran oceanic lithosphere in mantle magma genesis. Gabbroic intrusions and the great abundance of mafic to dioritic autoliths in tonalitic-granodioritic rocks provide evidence for mantle magma intervening in arc development. However, we suggest that upwelling mantle magmas represented much more a heat source triggering partial melting on the lower crust than a direct juvenile magma source for the arc.

Our studies show that rocks from the monzonitic suite (from monzogabbro to quartz monzonite, Fig. 3) mainly occur along the western zone of the arc, whilst rocks not so rich in potassium are more common from the central to eastern zones. Moreover, the calc-alkaline rocks of mafic composition are more common along the western zone of the arc (Gonçalves et al., 2010, 2014; Novo et al., 2010b; Tedeschi, 2013). This, together with the age distribution in space and time provide the guidelines for an evolutionary model (Fig. 14).

The U–Pb age histograms suggest three main age intervals and their peaks (Fig. 13). The oldest age interval, from 632 Ma to 605 Ma, shows a peak at 625-615 Ma. It follows an age interval from 605 Ma to 585 Ma, with a peak at 600–590 Ma. Finally, the youngest age interval, from 585 Ma to 570 Ma, shows a peak at 585–575 Ma (Fig. 13). Combining age relations shown in Figs. 2 and 13, the age distribution in space and time along the whole arc shows distinct patterns concerning each age interval. Ages from the oldest interval (632-605 Ma) tend to be concentrated in the eastern and central zones of the arc (Fig. 13B). Ages from the intermediate interval (605–585 Ma) are widespread along the whole arc, seeming to be more common from the central to the western zones (Figs. 2 and 13). Finally, the youngest ages (585–575 Ma) mostly occur from the central to the western zones of the Rio Doce arc.

The presented data suggest an evolutionary model for the Rio Doce magmatic arc, mostly based on its central sector, as follows (Fig. 14):

- ✓ Phase 1 - Subduction of oceanic lithosphere from west to east triggered the arc building processes along the (present-day) eastern zone of the Rio Doce arc, from ca. 632 to ca. 605 Ma.
- ✓ Phase 2 – Slab retreating and subduction of the ridge from ca. 605 Ma to ca. 585 Ma catalyzed the production of a large amount of magmas, shown by plutons widespread over all arc zones.
- ✓ Phase 3 – Slab break-off in the pre-collisional to collisional transition caused a heat input under the western arc zone, generating the late arc intrusions. This last arc development phase overlaps the early collisional stage of the Araçuaí orogen.

Acknowledgments

The authors are grateful to the Brazilian research and development agencies (CNPq, CAPES, CODEMIG, CPRM,) for financial support; to Frank Söllner, Richard Armstrong, and technical staffs of the geochronological laboratories of São Paulo, Brasília and Ouro Preto universities, for isotopic analyses; and to Umberto Cordani, Valdecir Janasi, Leonardo Alkmin and an anonymous reviewer, for suggestions that greatly improve the manuscript.

Appendix A. Supplementary data

Supplementary data related to this article can be found at http://dx.doi.org/10.1016/j.jsames.2015.11.011.

References

Alkmim, F.F., Marshak, S., Pedrosa-Soares, A.C., Peres, G.G., Cruz, S.C.P., Whittington, A., 2006. Kinematic evolution of the Araçuaí–West Congo orogen in Brazil and Africa: nutcracker tectonics during the Neoproterozoic assembly of

Gondwana. Precambrian Res. 149, 43–64.
Aracema, L.W., França, A.V.M., Pedrosa-Soares, A.C., Noce, C.M., Ferreira, D.C., 1999. Granitóides cálcio-alcalinos do arco magmático neoproterozóico da Faixa Araçuaí: evidências petrográficas e geoquímicas da região de Teófilo Otoni, MG, Brasil. In: Anais V Congresso Geoquímica dos Países de Língua Portuguesa, Porto Seguro, pp. 435–437.
Baltazar, O.F., Zucchetti, M., Oliveira, S.A.M., Scandolara, J., Silva, L.C., 2010. Projeto São Gabriel da Palha e Linhares, Estados do Espírito Santo e Minas Gerais: texto explicativo. Programa Geologia do Brasil. CPRM, Belo Horizonte, Brazil, p. 144.
Barbosa, A.L.de M., Grossi Sad, J.H., Torres, N., Melo, M.T.V., 1964. Geologia das quadrículas de Barra do Cuieté e Conselheiro Pena, Minas Gerais. DNPM/GEOSOL, Belo Horizonte, Brazil, p. 285.
Black, L.P., Kamo, S.L., Allen, C.M., Aleinikoff, J.N., Davis, D.W., Korsch, R.J., Foudoulis, C., 2003. TEMORA 1: a new zircon standard for Phanerozoic U-Pb geochronology. Chem. Geol. 200, 155–170.
Belém, J., 2014. Geoquímica, Geocronologia e contexto geotectônico do magmatismo máfico associado ao feixe de fraturas Colatina, Estado do Espírito Santo. Ph.D. thesis. Universidade Federal de Minas Gerais, Belo Horizonte, Brazil, p. 148.
Bento dos Santos, T., Munhá, J., Tassinari, C., Fonseca, P., 2011. The link between partial melting, granitization and granulite development in central Ribeira Fold Belt, SE Brazil: new evidence from elemental and Sr–Nd isotopic geochemistry. J. S. Am. Earth Sci. 31, 262–278.
Bento dos Santos, T.M., Tassinari, C.C.G., Fonseca, P.E., 2015. Diachronic collision, slab break-off and long-term high thermal flux in the Brasiliano-Pan-African orogeny: Implications for the geodynamic evolution of the Mantiqueira Province. Precambrian Res. 260, 1–22.
Campos-Neto, M.C., Figueiredo, M.C.H., 1995. The Rio doce orogeny, south-eastern Brazil. J. S. Am. Earth Sci. 8, 143–162.
Chappell, B.W., White, A.J.R., 2001. Two contrasting granite types: 25 years later. Aust. J. Earth Sci. 48, 489–499.
Chappell, B.W., Colleen, J.B., Doone, W., 2012. Peraluminous I-type granites. Lithos 153, 142–153.
Chemale, F., Kawashita, K., Dussin, I.A., Ávila, J.N., Justino, D., Bertotti, A., 2012. U-Pb zircon in situ dating with LA-MC-ICP-MS using a mixed detector configuration. An. Acad. Bras. Ciênc. 84, 275–295.
Chu, N.C., Taylor, R.N., Chavagnac, V., Nesbitt, R.W., Boella, R.M., Milton, J.A., German, C.R., Bayon, G., Burton, K., 2002. Hf isotope ratio analysis using multi-collector inductively coupled plasma mass spectrometry: an evaluation of isobaric interference corrections. J. Anal. Atomic Spectrom. 17, 1567–1574.
Cordani, U.G., Coutinho, J.M.V., Nutman, A.P., 2002. Geochronological constraints on the evolution of the Embu Complex. J. S. Am. Earth Sci. 14, 903–910.
Corrales, F.F.P., 2015. Geologia e Geocronologia do Complexo Marceleza: Vestígios de um arco magmático cordilherano no Terreno Paraíba do Sul, no limite entre os Estados do Rio de Janeiro e Minas Gerais. Master Thesis. Universidade do Estado do Rio de Janeiro, Rio de Janeiro, Brazil, p. 147.
De Campos, C., Mendes, J., Ludka, I., de Medeiros, S., de Moura, J., Wallfass, C., 2004. A review of the Brasiliano magmatism in southern Espírito Santo, Brazil, with emphasis on post-collisional magmatism. In: Weinberg, R., Trouw, R., Fuck, R., Hackspacher, P. (Eds.), The 750-550 Ma Brasiliano Event of South America. Journal of the Virtual Explorer, Electronic Edition Paper 1.
DePaolo, D.J., 1981. Neodymium isotopes in the Colorado front range and crust-mantle evolution in the Proterozoic. Nature 291, 193–196.
Figueiredo, C.M.S., 2009. O Arco Magmático Brasiliano na conexão entre os orógenos Araçuaí e Ribeira, Região de Muriaé-MG. Master Thesis. Universidade Federal de Minas Gerais, Belo Horizonte, Brazil, p. 103.
Figueiredo, M.C.H., Campos Neto, M.C., 1992. Geoquímica dos charnockitóides Serra do Valentim (ES). In: 37° Congresso Brasileiro de Geologia, São Paulo, Brazil, pp. 383–384.
Figueiredo, M.C.H., Campos Neto, M.C., 1993. Geochemistry of the Rio doce magmatic arc, Southeastern Brazil. An. Acad. Bras. Ciênc. 65, 63–81.
Frost, B.R., Arculus, R.J., Barnes, C.G., Collins, W.J., Ellis, D.J., Frost, C.D., 2001. A geochemical classification of granitic rocks. J. Petrol. 42, 2033–2048.
Gioia, S.M.C.L., Pimentel, M.M., 2000. The Sm-Nd isotopic method in the geochronology laboratory of the university of Brasília. An. Acad. Bras. Ciênc. 72, 219–245.
Gonçalves, L.E.S., 2009. Características gerais e história deformacional da Suíte Granítica G1, entre Governador Valadares e Ipanema, MG. Master Thesis. Universidade Federal de Ouro Preto, Ouro Preto, Brazil, p. 112.
Gonçalves, L. E. da S., Alkmim, F.F., Pedrosa-Soares, A.C., 2010. Características geoquímicas da Suíte G1, arco magmático do Orógeno Araçuaí, entre Governador Valadares e Ipanema, MG. Rev. Esc. Minas 63, 457–464.
Gonçalves, L., Farina, F., Lana, C., Pedrosa-Soares, A.C., Alkmim, F., Nalini, H.A., 2014. New U-Pb ages and lithochemical attributes of the ediacaran Rio Doce magmatic arc, araçuaí confined orogen, Southeastern Brazil. J. S. Am. Earth Sci. 52, 1–20.
Gonçalves, L., Alkmim, F., Pedrosa-Soares, A.C., Dussin, I.A., Valeriano, C.M., Lana, C., Tedeschi, M.F., 2015. Granites of the intracontinental termination of a magmatic arc: an example from the Ediacaran Araçuaí Orogen, Southeastern Brazil. Gondwana Res. http://dx.doi.org/10.1016/J.GR.2015.07.015.
Gonçalves-Dias, T., 2012. Caracterização geoquímica e geocronológica do Complexo Jequitinhonha na área-tipo, Orógeno Araçuaí. Master Thesis. Universidade Federal de Minas Gerais, Belo Horizonte, Brazil.
Gradim, C., Roncato, J., Pedrosa-Soares, A.C., Cordani, U., Dussin, I., Alkmim, F., Queiroga, G., Jacobson, T., Silva, L.C., Babinski, M., 2014. The hot back-arc zone of the Araçuaí orogen, Eastern Brazil: from sedimentation to granite generation. Braz. J. Geol. 44, 155–180.
Griffin, W.L., Pearson, N.J., Belousova, E.A., Saeed, A., 2006. Comment: Hf-isotope heterogeneity in zircon 91500. Chem. Geol. 233, 358–363.
Heilbron, M., Machado, N., 2003. Timing of terrane accretion in the Neoproterozoic-Eopaleozoic ribeira orogen (SE Brazil). Precambrian Res. 125, 87–112.
Heilbron, M., Almeida, J.C.H., Silva, L.G.E., Palermo, N., Tupinambá, M., Duarte, B.P., Valladares, C., Ramos, R.C., Ribeiro, A., Sanson, M., 2007. Geologia e Recursos Minerais das folhas Santa Rita do Jacutinga, Barra do Piraí, Volta Redonda e Angra dos Reis, escala 1:100.000. CPRM - MME, Brasília, Brazil, 1, p.177.
Heilbron, M., Valeriano, C.M., Tassinari, C.C.G., Almeida, J., Tupinambá, M., Siga, O., Trouw, R., 2008. Correlation of Neoproterozoic terranes between the Ribeira Belt, SE Brazil and its African counterpart: comparative tectonic evolution and open questions. Geol. Soc. Spec. Publ. 294, 211–237.
Heilbron, M., Duarte, B., Valeriano, C., Simonetti, A., Machado, N., Nogueira, J., 2010. Evolution of reworked Paleoproterozoic basement rocks within the Ribeira belt (Neoproterozoic), SE-Brazil, based on U Pb geochronology: implications for paleogeographic reconstructions of the São Francisco-Congo paleocontinent. Precambrian Res. 178, 136–148.
Heilbron, M., Tupinambá, M., Valeriano, C.M., Armstrong, R., Do Eirado Silva, L.G., Melo, R.S., Simonetti, A., Pedrosa-Soares, A.C., Machado, N., 2013. The Serra da Bolívia complex: the record of a new Neoproterozoic arc-related unit at Ribeira belt. Precambrian Res. 238, 158–175.
Hibbard, M.J., 1995. Petrography to Petrogenesis. Prentice Hall, New Jersey, p. 533.
Irvine, T.N., Baragar, W.R.A., 1971. A guide to the chemical classification of the common volcanic rocks. Can. J. Earth Sci. 8, 523–548.
Jackson, S.E., Pearson, N.J., Griffin, W.L., Belousova, E.A., 2004. The application of laser ablation–inductively coupled plasma–mass spectrometry to in situ U–Pb zircon geochronology. Chem. Geol. 211, 47–69.
Kuchenbecker, M., Pedrosa-Soares, A.C., Babinski, M., Fanning, M., 2015. Detrital zircon age patterns and provenance assessment for pre-glacial to post-glacial successions of the Neoproterozoic Macaúbas Group, Araçuaí orogen, Brazil. Precambrian Res. 266, 12–26.
Ludwig, K.R., 2001. User's Manual for Isoplot/Ex Version 2.49, a Geochronological Toolkit for Microsoft Excel. Berkeley Geochronological Center. Special Publication 1a, p. 55.
Ludwig, K.R., 2003. Using Isoplot/Ex, Version 3.00, a Geochronological Tool Kit for Microsoft Excel. Berkeley Geochronology Center. Special Publication 1, p.43.
Martins, V. T. de S., Teixeira, W., Noce, C.M., Pedrosa-Soares, A.C., 2004. Sr e Nd characteristics of Brasiliano/Pan-African granitoid plutons of the Araçuaí orogen, Southeastern Brazil: tectonic implications. Gondwana Res. 7, 75–89.
Mondou, M., Egydio, M., Vauchez, A., Raposo, M., Bruguier, O., Oliveira, A., 2012. Complex, 3D strain patterns in a synkinematic tonalite batholith from the Araçuaí Neoproterozoic orogen (Eastern Brazil): evidence from combined magnetic and isotopic chronology studies. J. Struct. Geol. 39, 158–179.
Morel, M.L.A., Nebel, O., Nebel-Jacobsen, Y.J., Miller, J.S., Vroon, P.Z., 2008. Hafnium isotope characterization of the GJ-1 zircon reference material by solution and Laser-Ablation MC-ICPMS. Chem. Geol. 255, 231–235.
Nalini Jr., H.A., 1997. Caractérisation des suítes magmatiques néoprotérozoiques de la region de Conselheiro Pena et Galiléia (Minas Gerais, Brésil). Etude géochimique et structurale des suítes Galiléia et Urucum et relations avec les pegmatites à éléments rares associées. Ph.D. thesis. École des Mines de Saint Etienne et École des Mines de Paris, France, p. 237.
Nalini Jr., H.A., Bilal, E., Paquette, J.L., Pin, C., Machado, R., 2000. Géochronologie U–Pb et géochimie isotopique Sr–Nd des granitoides neoproterozoiques des suites Galiléia et Urucum, vallée du Rio Doce, Sud-Est du Brésil. Comptes Rendus Acad. Sci. Paris 331, 459–466.
Nalini Jr., H.A., Machado, R., Bilal, E., 2005. Geoquímica e Petrogênese da Suíte Galiléia: exemplo de Magmatismo Tipo-I Metaluminoso Pré-Colisional Neoproterozóico da Região do Médio Vale do Rio Doce (MG). Rev. Bras. Geociênc. 35, 23–34.
Noce, C.M., Macambira, M.B., Pedrosa-Soares, A.C., 2000. Chronology of Neoproterozoic Cambrian granitic magmatism in the Araçuaí Belt, Eastern Brazil, based on single zircon evaporation dating. Rev. Bras. Geociênc. 30, 25–29.
Noce, C.M., Romano, A.W., Pinheiro, C.M., Mol, V.S., Pedrosa-Soares, A.C., 2003. Geologia das Folhas Ubá e Muriaé. In: Pedrosa-Soares, A.C., Noce, C.M., Trouw, R., Heilbron, M. (Eds.), Projeto Sul de Minas – Etapa I: Geologia e Recursos Minerais do Sudeste Mineiro, 12. COMIG/UFMG/UFRJ/UERJ, Belo Horizonte, Brazil, pp. 623–659.
Noce, C.M., Pedrosa-Soares, A.C., Silva, L.C., Armstrong, R., Piuzana, D., 2007a. Evolution of polyciclic basement complexes in the Araçuaí orogen, based on U-Pb SHRIMP data: Implications for Brazil-Africa links in Paleoproterozoic time. Precambrian Res. 159, 60–78.
Noce, C.M., Pedrosa-Soares, A.C., Silva, L.C., Alkmim, F.F., 2007b. O Embasamento Arqueano e Paleoproterozóico do Orógeno Araçuaí. Geonomos 15, 17–23.
Novo, T., Noce, C.M., Pedrosa-Soares, A.C., Figueiredo, C., 2010a. Geologia e Recursos Minerais da Folha Carangola SE.23-X-B-VI. CPRM-Serviço Geológico do Brasil, Belo Horizonte, Brazil, p. 72.
Novo, T., Pedrosa-Soares, A.C., Noce, C.M., Alkmim, F.F., Dussin, I., 2010b. Rochas charnockíticas do sudeste de Minas Gerais: a raiz granulítica do arco Magmático do Orógeno Araçuaí. Rev. Bras. Geociênc. 40, 573–592.
Novo, T., 2013. Caracterização do Complexo Pocrane, magmatismo básico mesoproterozóico e unidades neoproterozóicas do sistema Araçuaí-Ribeira, com ênfase em geocronologia U-Pb (SHRIMP e LA-ICP-MS). Universidade Federal de Minas Gerais, Belo Horizonte, Brazil, p. 193.

Paes, V.J.C., Raposo, F.O., Pinto, C.P., Oliveira, F.A.R., 2010. Projeto Jequitinhonha, Estados de Minas Gerais e Bahia: texto explicativo. Geologia e Recursos Minerais das Folhas Comercinho, Jequitinhonha, Almenara, Itaobim, Joaíma e Rio do Prado. Programa Geologia do Brasil. CPRM, Belo Horizonte, Brazil, p. 376.
Patchett, P.J., Tatsumoto, M., 1980. A routine high-precision method for Lu-Hf isotope geochemistry and chronology. Contrib. Mineral. Petrol. 75, 263–267.
Pearce, J.A., Harris, N., Tindle, A., 1984. Trace element discrimination diagrams for the tectonic interpretation of granitic rocks. J. Petrol. 259, 956–983.
Pedrosa-Soares, A.C., Noce, C.M., Vidal, P.H., Monteiro, R.L.B.P., Leonardos, O.H., 1992. Toward a new tectonic model for the late proterozoic araçuaí (SE-Brazil) – west Congolian (SW africa) Belt. J. S. Am. Earth Sci. 6, 33–47.
Pedrosa-Soares, A.C., Vidal, P., Leonardos, O.H., Brito-Neves, B.B., 1998. Neoproterozoic oceanic remnants in eastern Brazil: further evidence and refutation of an exclusively ensialic evolution for the Araçuaí-West Congo orogeny. Geology 26, 519–522.
Pedrosa-Soares, A.C., Noce, C.M., Wiedemann, C.M., Pinto, C.P., 2001. The Araçuaí-West Congo orogen in Brazil: an overview of a confined orogeny formed during Gondwanaland assembly. Precambrian Res. 110, 307–323.
Pedrosa-Soares, A.C., Noce, C.M., Trouw, R., Heilbron, M., 2003. Geologia e Recursos Minerais do Sudeste Mineiro. Projeto Sul de Minas, 1000. COMIG, Belo Horizonte, p. 822. http://www.portalgeologia.com.br.
Pedrosa-Soares, A.C., Noce, C.M., Alkmim, F.F., Silva, L.C., Babinski, M., Cordani, U., Castañeda, C., 2007. Orógeno Araçuaí: síntese do conhecimento 30 anos após Almeida 1977. Geonomos 15, 1–16.
Pedrosa-Soares, A.C., Alkmim, F.F., Tack, L., Noce, C.M., Babinski, M., Silva, L.C., Martins-Neto, M.A., 2008. Similarities and differences between the Brazilian and African counterparts of the Neoproterozoic Araçuaí-West Congo orogeny. In: Pankhurst, R.J., Trouw, R.A.J., Brito Neves, B.B., De Wit, M.J. (Eds.), West Gondwana: Pre-cenozoic Correlations across the South Atlantic Region, 294. Geological Society, London, pp. 153–172. Special Publications.
Pedrosa-Soares, A.C., De Campos, C.P., Noce, C.M., Silva, L.C., Novo, T., Roncato, J., Medeiros, S., Castañeda, C., Queiroga, G., Dantas, E., Dussin, I., Alkmim, F.F., 2011. Late Neoproterozoic-Cambrian granitic magmatism in the araçuaí orogen (Brazil), the eastern Brazilian Pegmatite province and related Mineral resources. In: Sial, A.N., Bettencourt, J.S., De Campos, C.P., Ferreira, V.P. (Eds.), Granite-related Ore Deposits, 350. Geological Society, London, pp. 25–51. Special Publications.
Peixoto, E., Pedrosa-Soares, A.C., Alkmim, F.F., Dussin, I.A., 2015. A suture–related accretionary wedge formed in the Neoproterozoic Araçuaí orogen (SE Brazil) during Western Gondwanaland assembly. Gondwana Res. 27, 878–896.
Petitgirard, S., Vauchez, A., Egydio-Silva, M., Bruguier, O., Campos, P., Monié, P., Babinski, M., Mondou, M., 2009. Conflicting structural and geochronological data from the Ibituruna quartz-syenite (SE Brazil): Effect of protracted 'hot' orogeny and slow cooling rate? Tectonophysics 477, 174–196.
Pinto, C.P., Drumond, J.B.V., Féboli, W.L., 2001. Projeto Leste. CPRM/CODEMIG, Belo Horizonte, Brazil (CD-ROM).
Queiroga, G.N., 2010. Caracterização de restos de litosfera oceânica do Orógeno Araçuaí entre os paralelos 17° e 21° S. Ph.D. thesis. Universidade Federal de Minas Gerais, Belo Horizonte, p. 180.
Queiroga, G., Pedrosa-Soares, A.C., Noce, C.M., Alkmim, F.F., Pimentel, M.M., Dantas, E., Martins, M., Castañeda, C., Suita, M.T.F., Prichard, F., 2007. Age of the Ribeirão da Folha ophiolite, Araçuaí orogen: the U–Pb zircon dating of a plagiogranite. Geonomos 15, 61–65.
Rickwood, P.C., 1989. Boundary lines within petrologic diagrams which use oxides of major and minor elements. Lithos 22, 247–263.
Schmitt, R.S., Trouw, R.A.J., Van Schmus, W.R., Passchier, C.W., 2008. Cambrian orogeny in the Ribeira Belt (SE Brazil) and correlations within West Gondwana: ties that bind underwater. J. Geol. Soc. Lond. 294, 279–296.
Shand, S.J., 1943. Eruptive Rocks. D. Van Nostrand Company, New York, p. 360.
Silva, L.C., Armstrong, R., Noce, C.M., Carneiro, M., Pimentel, M., Pedrosa-Soares, A.C., Leite, C., Vieira, V.S., Silva, M., Paes, V., Cardoso-Filho, J., 2002. Reavaliação da evolução geológica em terrenos pré-cambrianos brasileiros com base em novos dados U-Pb SHRIMP, parte II: Orógeno Araçuaí, Cinturão Móvel Mineiro e Cráton São Francisco Meridional. Rev. Bras. Geociênc. 32, 513–528.
Silva, L.C., McNaughton, N.J., Armstrong, R., Hartmann, L., Fletcher, I., 2005. The Neoproterozoic Mantiqueira Province and its African connections. Precambrian Res. 136, 203–240.
Silva, L.C., Pedrosa-Soares, A.C., Armstrong, R., Noce, C.M., 2011. Determinando a duração do período colisional do Orógeno Araçuaí com base em geocronologia U-Pb de alta resolução em zircão: uma contribuição para a história da amalgamação do Gondwana Ocidental. Geonomos 19, 180–197.
Sláma, J., Košler, J., Condon, D.J., Crowley, J.L., Gerdes, A., Hanchar, J.M., Horstwood, M.S.A., Morris, G.A., Nasdala, L., Norberg, N., Schaltegger, U., Schoene, B., Tubrett, M.N., Whitehouse, M.J., 2008. Plešovice zircon - A new natural reference material for U-Pb and Hf isotopic microanalysis. Chem. Geol. 249, 1–35.
Sluitner, Z., Weber-Diefenbach, K., 1989. Geochemistry of charnoenderbitic granulites and associated amphibolitic gneisses in the coast region of Espírito Santo, Brazil. Zent. Geol. Paleontol. Teil I H. 5/6, 917–931.
Söllner, F., Lammerer, B., Weber-Diefenbach, K., 1989. Brasiliano age of a charnoenderbitic rock suite in the Complexo Costeiro (Ribeira Mobile Belt), Espirito Santo, Brazil: evidence from U-Pb geochronology on zircons. Zent. Geol. Paleontol. Teil I H 5/6, 933–945.
Tedeschi, M., 2013. Caracterização do arco magmático do Orógeno Araçuaí entre Frei Inocêncio e Itambacuri, Minas Gerais. Master Thesis. Universidade Federal de Minas Gerais, Belo Horizonte, Brazil, p. 126.
Trouw, R.A.J., Peternel, R., Ribeiro, A., Heilbron, M., Vinagre, R., Duffles, P., Trouw, C.C., Fontainha, M., Kussama, H.H., 2013. A new interpretation for the interference zone between the southern Brasília belt and the central Ribeira belt, SE Brazil. J. S. Am. Earth Sci. 48, 43–57.
Tupinambá, M., Heilbron, M., Valeriano, C., Porto Jr., R., Dios, F.B., Machado, N., Silva, Eirado Silva, L., Almeida, J., 2012. Juvenile contribution of the Neoproterozoic Rio Negro Magmatic Arc (Ribeira Belt, Brazil): Implications for Western Gondwana amalgamation. Gondwana Res. 21, 422–438.
Tupinambá, M., Heilbron, M., Duarte, B.P., Nogueira, J.R., Valladares, C., Almeida, J.C.H., Eirado-Silva, L.G.E., Medeiros, S.R., Almeida, C.G., Miranda, A., Ragatky, C.D., Mendes, J.C., Ludka, I., 2007. Geologia da Faixa Ribeira Setentrional: Estado da Arte e Conexões com a Faixa Araçuaí. Geonomos 15, 67–79.
Tupinambá, M., Almeida, C., Eirado, E., Duarte, B., Heilbron, M., 2002. Geologia da Folha Pirapetinga (SF.23-X-D-VI). Projeto Sul de Minas. CODEMIG, Belo Horizonte, Brazil (CD-ROM).
Valeriano, C.M., Tupinambá, M., Simonetti, A., Heilbron, M., Almeida, J.C.H., do Eirado, L.G., 2011. U-Pb LA-MC-ICPMS geochronology of Cambro-Ordovician post-collisional granites of the Ribeira belt, southeast Brazil: Terminal Brasiliano magmatism in central Gondwana supercontinent. J. S. Am. Earth Sci. 32, 416–428.
Vieira, V.S., 1993. Folha Baixo Guandu (SE.24-Y-C-V). Programa Levantamentos Geológicos Básicos do Brasil. DNPM/CPRM, Brasília, Brazil.
Vieira, V.S., 2007. Significado do Grupo Rio Doce no Contexto do Orógeno Araçuaí. Ph.D. thesis. Universidade Federal de Minas Gerais, Belo Horizonte, Brazil, p. 117.
Whittington, A.G., Connelly, J., Pedrosa-Soares, A.C., Marshak, S., Alkmim, F.F., 2001. Collapse and melting in a confined orogenic belt: preliminary results from the Neoproterozoic Aracuai belt of eastern Brazil. In: American Geophysical Union, AGU Fall Meeting, Abstracts, T32B–089, 82, pp. 1181–1182.
Wiedemann, C.M., Medeiros, S.R., Mendes, J.C., Ludka, I.P., Moura, J.C., 2002. Architecture of late orogenic plutons in the Araçuaí–Ribeira folded belt, southeast Brazil. Gondwana Res. 5, 381–399.
Wilson, M., 1989. Igneous Petrogenesis. A Global Tectonic Approach. Unwin Hyman, London, p. 466.
Wu, F.Y., Yang, Y.H., Xie, L.W., Yang, J.H., Xu, P., 2006. Hf isotopic compositions of the standard zircons and baddeleyites used in U–Pb geochronology. Chem. Geol. 234, 105–126.